Mathematical Biosciences 377 (2024) 109301

Contents lists available at ScienceDirect

Mathematical Biosciences

journal homepage: www.elsevier.com/locate/mbs

Original Research Article

A joint-threshold Filippov model describing the effect of intermittent androgen-deprivation therapy in controlling prostate cancer

Aili Wang [a], Rong Yan [b], Haixia Li [b], Xiaodan Sun [c], Weike Zhou [d], Stacey R. Smith? [e,*]

[a] School of Science, Xi'an University of Technology, Xi'an 710054, PR China
[b] School of Mathematics and Information Science, Baoji University of Arts and Sciences, Baoji 721013, PR China
[c] School of Mathematics and Statistics, Xi'an Jiaotong University, Xi'an 710049, PR China
[d] School of Mathematics, Northwest University, Xi'an, Shaanxi 710127, PR China
[e] Department of Mathematics and Faculty of Medicine, The University of Ottawa, Ottawa, ON K1N 6N5, Canada

ARTICLE INFO

Keywords:
Filippov model
Prostate cancer
Joint threshold
Intermittent deprivation therapy
Sliding dynamics
Sliding bifurcation

ABSTRACT

Intermittent androgen-deprivation therapy (IADT) can be beneficial to delay the occurrence of treatment resistance and cancer relapse compared to the standard continuous therapy. To study the effect of IADT in controlling prostate cancer, we developed a Filippov prostate cancer model with a joint threshold function: therapy is implemented once the total population of androgen-dependent cells (AC-Ds) and androgen-independent cells (AC-Is) is greater than the threshold value ET, and it is suspended once the population is less than ET. As the parameters vary, our model undergoes a series of sliding bifurcations, including boundary node, focus, saddle, saddle-node and tangency bifurcations. We also obtained the coexistence of one, two or three real equilibria and the bistability of two equilibria. Our results demonstrate that the population of AC-Is can be contained at a predetermined level if the initial population of AC-Is is less than this level, and we choose a suitable threshold value.

1. Introduction

Prostate cancer, one of the most common forms of malignant cancer, is the second leading cause of cancer-related mortality in men in the global north [1]. Approximately one in six men are diagnosed with prostate cancer. The average five-year survival rate of prostate cancer is about 99%, dropping to 30% after the cancer metastasizes. Although the rate of prostate-cancer progression is very slow, the incidence of prostate cancer keeps increasing worldwide [2,3]. In 1941, Huggins demonstrated that castration induces the regression of prostate tumours, suggesting high dependence of prostate cancer cells on androgen, a male-characteristic hormone similar to testosterone [4]. Therefore, androgen-deprivation therapy (ADT) — a type of hormonal therapy inhibiting prostate cancer cell proliferation, promoting the death of prostate cancer cells and preventing prostate cancer cells' mutation — has become the most commonly used method to treat prostate cancer [5]. However, ADT was initially administrated continuously, known as continuous androgen-deprivation therapy (CADT), which is often associated with such side effects as impotence, depression, bone demineralization, dementia and even therapy resistance [6–8]. Intermittent androgen-deprivation therapy (IADT), which consists of patients going on and off therapy according to either a prostate-specific antigen threshold or a fixed time interval, has been proposed as an alternative to CADT to reduce the side effects, which can significantly improve patients' quality of life [9,10].

Since the effect of the therapy and the mechanism of prostate cancer is far from understood, mathematical models have been proposed to better explain the observation from experimental and clinical studies [11–22]. To identify the models with the highest likelihood to mimic the clinically observed dynamics, Pasetto et al. performed Bayesian inference and model calibration in order to determine the treatment schedule of hormone therapy [11,12]. Kuang et al. focused on the modelling and parameterization of the progression dynamics of prostate cancer during the implementation of ADT [13–16]. Wang et al. studied the dynamics of prostate-cancer models with ADT in which the different competition intensities between AC-Ds and AC-Is was mimicked [17–19]. Pei et al. modelled the impact of intermittent therapy on the development of the tumour cells by formulating impulsive models, which include the residual effect of chemotherapy [20,21]. They found that optimal IADT plus chemotherapy can greatly reduce the on-treatment time, as well as the level of prostate-specific antigen. Hirata et al. found that intermittent androgen suppression cannot stabilize the origin (where no cancer cells exist for some patients), so they highlighted the importance of seeking to delay the relapse [23].

* Corresponding author.
E-mail addresses: wangal@xaut.edu.cn (A. Wang), stacey.smith@uottawa.ca (S.R. Smith?).

https://doi.org/10.1016/j.mbs.2024.109301
Received 3 March 2024; Received in revised form 20 August 2024; Accepted 9 September 2024
Available online 20 September 2024

Cunningham et al. applied evolutionary game theory to mimic evolution within a patient, and the best therapy schedule was explored based on optimal control theory [22]. Adamiecki et al. reviewed the literature of *in vitro*, *ex vivo* and *in vivo* models of prostate cancer, in order to help tackle the question of which model associated with the development of prostate cancer best suits their future studies [24,25]. Many of the existing models account for the interaction between AC-Ds and AC-Is, the microenvironment of inter-patients, the acquisition of therapy resistance and the efficacy of treatments. Most modelling work considering the effects of ADT assumes that ADT is administrated continuously or is activated following a fixed time interval. There are limitations to these studies, although ADT has been revealed to make crucial contributions to tumour inhibition and yields useful insights on the treatment of prostate cancer.

In order to examine the effect of intermittent therapy, Filippov models have been proposed. These models are continuous but have discontinuities in the derivatives, which have been shown to correspond to delays in the application of interventions [26]. Filippov models include multiple subsystems with different dynamics that are distinguished by the value of the adjoining thresholds [27,28]; such models can improve on impulsive models and classic continuous models. Here, we adopt a Filippov model with a single threshold to mimic the impact of IADT on the evolution of the prostate cancer, in order determine when to administer the treatment as determined by the population of AC-Ds [29]. Ideally, the populations of AC-Ds and AC-Is could be detected separately, resulting in a single threshold strategy dependent on AC-D population. However, it is difficult to measure the population of these two cancer cells independently, so a joint threshold is required. The control strategy with a joint threshold is defined as follows: when the sum of the population of AC-Ds and AC-Is exceeds a certain level, the therapy is activated; otherwise, the therapy is suspended.

Filippov systems have been successfully applied in plant diseases [30], pest management [31–33] and epidemic control [34–38], including modelling the spread of HIV and COVID-19 [39,40], and there are various results on the dynamics of Filippov systems with a single threshold. However, there are still very few results for the dynamics of Filippov systems with more complex threshold functions or generalized threshold functions [41–43]. We address the question of how to analyse the dynamics of Filippov system with a joint threshold and find effective ADT schedules for prostate cancer. The organization of our paper is as follows: In Section 2, we establish a Filippov model of prostate cancer cells with joint threshold function and analyse the dynamics of the subsystems. In Section 3, we explore the sliding-mode region as well as the sliding dynamics. The sliding bifurcation, including boundary-equilibrium bifurcation and tangency bifurcation, and global dynamics will be addressed in Section 4. We present a discussion in the last section.

2. A Filippov prostate cancer model with joint threshold

We assume that whether ADT is implemented depends not only on the population of AC-Ds but also on that of AC-Is, which owes to the fact that it is hard to measure the population of AC-Ds and AC-Is individually. This induces a joint threshold that depends on both AC-D and AC-I populations. Therefore, we established a novel model with joint threshold by improving our previous model [29]. The joint threshold is defined as follows: ADT is implemented once the total population of AC-Ds and AC-Is is greater than the threshold value ET; the therapy is suspended once the total population of AC-Ds and AC-Is is less than this threshold. ADT has three main effects for prostate cancer: inhibiting prostate-cancer-cell proliferation, accelerating cell mortality and preventing cell mutation. Thus we established the following Filipov prostate cancer model:

$$\begin{aligned}\frac{dX_1}{dt} &= r_1(1-\epsilon u)\left(1-\frac{X_1+\alpha X_2}{K}\right)X_1-(d_1+m_1)\epsilon u X_1,\\ \frac{dX_2}{dt} &= r_2\left(1-\frac{\beta X_1+X_2}{K}\right)X_2+m_1 u\epsilon X_1,\end{aligned} \tag{1}$$

with

$$\epsilon=\begin{cases}0, & \sigma(X_1,X_2)\equiv X_1+X_2-ET<0,\\ 1, & \sigma(X_1,X_2)\equiv X_1+X_2-ET>0,\end{cases} \tag{2}$$

where X_1 represents the population of AC-Ds and X_2 represents the population of AC-Is, r_1 denotes the growth rate of AC-Ds, d_1 denotes ADT-induced mortality rate of AC-Ds, r_2 represents the net growth rate of AC-Is, K is the carrying capacity of cancer cells, α and β represent the positive competition coefficients between AC-Ds and AC-Is, m_1 represents the irreversible mutation rate from AC-Ds to AC-Is and u is the efficacy of ADT for prostate cancer. In model (1)–(2), $\sigma(X_1,X_2)$ is a joint threshold function, which depends on the sum of the population of AC-Ds and AC-Is; i.e., $\sigma(X_1,X_2)=X_1+X_2-ET$, and ϵ is a discontinuous control function. The detailed definitions and values of each parameter are as shown in Table 1. It is worth noting that our targeted model (1)–(2) is a non-smooth model with discontinuous right-hand sides, which mimics the situation where activating or suspending ADT depends on the total population of the AC-Ds and AC-Is. However, the model that Pei et al. formulated is a piecewise one with pulsed pattern, in which on-treatment and off-treatment processes are activated at fixed moments [20]. The model that Hirata et al. studied is piecewise linear, and its dynamics are modelled with rapid shifts between two levels according to fixed intervals [23]. It follows that a substantial difference exists between the targeted model proposed in this work and the above models.

In the following, we define the hyperplane

$$\Sigma\equiv\left\{(X_1,X_2)\in R_+^2\,\middle|\,\sigma(X_1,X_2)=0\right\}$$

separating $\mathbb{R}_+^2$ into two regions:

$$G_1\equiv\left\{(X_1,X_2)\in R_+^2\,\middle|\,\sigma(X_1,X_2)<0\right\},$$

$$G_2\equiv\left\{(X_1,X_2)\in R_+^2\,\middle|\,\sigma(X_1,X_2)>0\right\}.$$

In region G_i, system (1)–(2) is denoted as $F_{G_i}(X)$; the components of $F_{G_i}(X)$ are denoted as F_{i1} and F_{i2}, where $i=1,2$. Letting $Z=(X_1,X_2)^T$, we get

$$F_{G_1}(Z)=\left(r_1\left(1-\frac{X_1+\alpha X_2}{K}\right)X_1,\quad r_2\left(1-\frac{\beta X_1+X_2}{K}\right)X_2\right)^T,$$

$$\begin{aligned}F_{G_2}(Z)=\Bigg(&r_1(1-u)\left(1-\frac{X_1+\alpha X_2}{K}\right)X_1-(d_1+m_1)uX_1,\\ &r_2\left(1-\frac{\beta X_1+X_2}{K}\right)X_2+m_1uX_1\Bigg)^T.\end{aligned}$$

Then system (1)–(2) constitutes the following Filippov system:

$$\dot{Z}=\begin{cases}F_{G_1}(Z), & Z\in G_1,\\ F_{G_2}(Z), & Z\in G_2.\end{cases} \tag{3}$$

We denote the Filippov system in the region G_1 as Subsystem S_1, and the Filippov system in the region G_2 as Subsystem S_2. Therefore, the dynamics of Filippov system (3) consist of the dynamics of Subsystems S_1 and S_2 and the dynamics on the hyperplane Σ.

Note that the trajectory of the Filippov system (3) consists of the standard trajectory in each region G_i $(i=1,2)$ and the sliding trajectory on Σ. To deal with the trajectory of the Filippov system (3) through a point $Z\in\Sigma$, we split Σ into three parts, depending on whether or not the vector field points towards it:

- crossing-mode region: $\Sigma_c=\{Z\in\Sigma|F_{G_1}\sigma(Z)\cdot F_{G_2}\sigma(Z)>0\}$,
- sliding-mode region: $\Sigma_s=\{Z\in\Sigma|F_{G_1}\sigma(Z)>0,\ F_{G_2}\sigma(Z)<0\}$,
- escaping-mode region: $\Sigma_e=\{Z\in\Sigma|F_{G_1}\sigma(Z)<0,\ F_{G_2}\sigma(Z)>0\}$.

Here $F_{G_i}(Z)\sigma(Z)=F_{G_i}(Z)\cdot\nabla\sigma(Z)$ $(i=1,2)$ is the Lie derivative of $\sigma(Z)=X_1+X_2-ET$ at point Z on the vector field F_{G_i}.

It is worth emphasizing that the sliding-mode region plays an important role in the dynamics of the Filippov system (3). Mathematically,

Table 1
Definitions and values of parameters for model (1)–(2).

Parameters	Definition	Value	Source
r_1	Growth rate of AC-Ds	0.5/day	[13]
d_1	Mortality rate of AC-Ds	0.064/day	[13]
r_2	Net growth rate of AC-Is	0.006/day	[13]
m_1	Irreversible mutation rate from AC-Ds to AC-Is	0.00005/day	[19]
K	Cancer cell carrying capacity	11 billion	[13]
u	Efficacy of ADT for prostate cancer	0.5	[17]
α, β	Positive competition coefficients between AC-Ds and AC-Is	varied	–

once a trajectory reaches the sliding-mode region, it will slide along this region. Biologically, in the sliding-mode region, there is a rapid alternation between implementing ADT and suspending ADT, resulting in shorter periods of both modalities.

In the following, we define three types of equilibria and two types of tangencies of Filippov system (3), which will be used in the rest of this paper.

Definition 1. (i) A point Z^* is called a *real equilibrium* of (3) if $F_{G_1}(Z^*) = 0, \sigma(Z^*) < 0$, or $F_{G_2}(Z^*) = 0, \sigma(Z^*) > 0$.

(ii) A point Z^* is called a *virtual equilibrium* of (3) if $F_{G_1}(Z^*) = 0, \sigma(Z^*) > 0$, or $F_{G_2}(Z^*) = 0, \sigma(Z^*) < 0$.

A real equilibrium is an equilibrium belonging to the region it lies in, which has not been excised. A virtual equilibrium is an equilibrium in a region that has been excised due the to Filippov definition, but which may still attract trajectories from another region. Both the real equilibrium and virtual equilibrium are called regular equilibria.

Let $\hat{F}(Z) = qF_{G_1}(Z) + (1-q)F_{G_2}(Z)$ be the convex combination of the two vectors $F_{G_1}(Z)$ and $F_{G_2}(Z)$ to each nonsingular point $Z \in \Sigma_s$, where

$$q = \frac{F_{G_2}(Z)\sigma(Z)}{\Big(F_{G_2}(Z) - F_{G_1}(Z)\Big)\sigma(Z)}.$$

Thus the sliding-mode dynamics of Filippov system (3) can be determined by

$$\frac{\mathrm{d}Z}{\mathrm{d}t} = \hat{F}(Z), \qquad Z \in \Sigma_s, \tag{4}$$

which is smooth on the sliding-mode region Σ_s.

Definition 2. A point Z^* is called a pseudo-equilibrium of Filippov system (3) if it is an equilibrium of the system (4).

Definition 3. A point Z^* is called a boundary equilibrium of Filippov system (3) if $F_{G_1}(Z^*) = 0, \sigma(Z^*) = 0$, or $F_{G_2}(Z^*) = 0, \sigma(Z^*) = 0$.

Definition 4. A point Z^* is called a tangency point of Filippov system (3) if $Z^* \in \Sigma$ and $F_{G_1}\sigma(Z^*) = 0$ or $F_{G_2}\sigma(Z^*) = 0$.

Such points are not equilibria of any individual region but are rather formed by the boundaries of Filippov regions. Note that $X_1 + X_2 = ET$ holds true in (4), so (4) is in fact of dimension one. Thus the stability of the pseudo-equilibrium can be derived by the sign of the function on the right-hand side of (4). If a pseudo-equilibrium of Filippov system (3) is stable, the population of the prostate cancer cells can be contained at a predetermined level, which can be pivotal in the treatment of prostate cancer.

2.1. Dynamics of subsystem S_1

Free-subsystem. When $X_1+X_2 < ET$ (i.e., $\epsilon = 0$), ADT is suspended and system (3) takes the following form:

$$\begin{aligned} \frac{dX_1}{dt} &= r_1\left(1 - \frac{X_1 + \alpha X_2}{K}\right)X_1, \\ \frac{dX_2}{dt} &= r_2\left(1 - \frac{\beta X_1 + X_2}{K}\right)X_2. \end{aligned} \tag{5}$$

We call system (5) the *free-subsystem.*

For subsystem S_1, we have a trivial equilibrium $E_0 = (0,0)$, two boundary equilibria $E_{01} = (0,K), E_{10} = (K,0)$ and a positive equilibrium $E_1^I = (X_{11}, X_{21}) = \left(\frac{(1-\alpha)K}{1-\alpha\beta}, \frac{(1-\beta)K}{1-\alpha\beta}\right)$. The following four cases illustrate the existence and stability of equilibria for the free-subsystem (5):

Case A_1: $\alpha < 1, \beta < 1$. There exist four equilibria $E_1^I, E_0, E_{01}, E_{10}$ for the free-subsystem (5); the regular equilibrium E_1^I is a stable node, E_0 is an unstable node, and both E_{01} and E_{10} are saddles.

Case A_2: $\alpha < 1, \beta > 1$. There exist three equilibria E_0, E_{01}, E_{10} for the free-subsystem (5); E_0 is an unstable node, E_{01} is a saddle and E_{10} is a stable node.

Case A_3: $\alpha > 1, \beta < 1$. There exist three equilibria E_0, E_{01}, E_{10} for the free-subsystem (5); E_0 is an unstable node, E_{01} is a stable node and E_{10} is a saddle.

Case A_4: $\alpha > 1, \beta > 1$. There exist four equilibria $E_1^I, E_0, E_{01}, E_{10}$ for the free-subsystem (5); the regular equilibrium E_1^I is a saddle, E_0 is an unstable node, and both E_{01} and E_{10} are stable nodes.

2.2. Dynamics of subsystem S_2

Control-subsystem. When $X_1+X_2 > ET$ (i.e., $\epsilon = 1$), ADT is carried out. The therapy will affect the proliferation rate, the mortality rate and the mutation rate of AC-Ds, so the following system can be used to describe the changes in the population of AC-Ds and AC-Is:

$$\begin{aligned} \frac{dX_1}{dt} &= r_1(1-u)\left(1 - \frac{X_1 + \alpha X_2}{K}\right)X_1 - (d_1 + m_1)uX_1, \\ \frac{dX_2}{dt} &= r_2\left(1 - \frac{\beta X_1 + X_2}{K}\right)X_2 + m_1uX_1. \end{aligned} \tag{6}$$

We call system (6) the *control-subsystem*. System (6) has an unstable trivial equilibrium $E_0 = (0,0)$, a boundary equilibrium $E_{01} = (0,K)$ and five possible positive equilibria:

(i) When $\alpha < Q, \alpha\beta \neq 1$, there exists one positive equilibrium E_1^{II};

(ii) When $\alpha > Q, \alpha\beta > 1, -\frac{A_2}{2A_1} < \frac{KQ}{\alpha}, \Delta_1 > 0$, there exist two positive equilibria E_1^{II} and E_2^{II};

(iii) When $\alpha > Q, \alpha\beta > 1, -\frac{A_2}{2A_1} < \frac{KQ}{\alpha}, \Delta_1 = 0$, there exists one positive equilibrium E_3^{II};

(iv) When $\alpha < Q, \alpha\beta = 1$, there exists one positive equilibrium E_4^{II};

(v) When $\alpha = Q, \alpha\beta > 1, \alpha m_1 u < r_2(\alpha\beta - 1)$, there exists one positive equilibrium E_5^{II}, where

$$E_1^{II} = (X_1^1, X_2^1) = \left(KQ - \alpha X_2^1, \frac{-A_2 - \sqrt{\Delta_1}}{2A_1}\right),$$

$$E_2^{II} = (X_1^2, X_2^2) = \left(KQ - \alpha X_2^2, \frac{-A_2 + \sqrt{\Delta_1}}{2A_1}\right),$$

$$E_3^{II} = (X_1^3, X_2^3) = \left(KQ - \alpha X_2^3, \frac{-A_2}{2A_1}\right),$$

$$E_4^{II} = (X_1^4, X_2^4) = \left(KQ + \alpha\frac{A_3}{A_2}, -\frac{A_3}{A_2}\right),$$

$$E_5^{II} = (X_1^5, X_2^5) = \left(\left(1 - \frac{\alpha m_1 u}{r_2(\alpha\beta - 1)}\right)\alpha K, \frac{\alpha m_1 u}{r_2(\alpha\beta - 1)}K\right),$$

and

$$Q = 1 - \frac{(d_1 + m_1)u}{r_1(1-u)}, \quad A_1 = r_2(\alpha\beta - 1), \quad A_2 = r_2K(1-\beta Q) - \alpha m_1 uK,$$
$$A_3 = m_1 uK^2 Q, \qquad \Delta_1 = A_2^2 - 4A_1A_3.$$

We summarize the existence and stability of all possible equilibria for system S_2 and have the following three cases.

Case B: $\alpha < Q$. In this case, we have two scenarios depending on the relationship between $\alpha\beta$ and 1.

Case B_1: When $\alpha < Q$ and $\alpha\beta \neq 1$, there exist three equilibria E_1^{II}, E_0 and E_{01}; the regular equilibrium E_1^{II} is a stable node or focus, E_0 is an unstable node and the equilibrium E_{01} is a saddle.

Case B_2: When $\alpha < Q$ and $\alpha\beta = 1$, there exist three equilibria E_4^{II}, E_0 and E_{01}; the regular equilibrium E_4^{II} is a stable node or focus, E_0 is an unstable node and the equilibrium E_{01} is a saddle.

Case C: $\alpha > Q$. In this case, there are three scenarios to consider.

Case C_1: When $\alpha > Q, \alpha\beta > 1, -\frac{A_2}{2A_1} < \frac{KQ}{\alpha}$ and $A_2^2 - 4A_1A_3 > 0$, there exist four equilibria E_1^{II}, E_2^{II}, E_0 and E_{01}; the regular equilibrium E_1^{II} is a stable node or focus, the regular equilibrium E_2^{II} is a saddle, E_0 is an unstable node and the equilibrium E_{01} is a stable node.

Case C_2: When $\alpha > Q, \alpha\beta > 1, -\frac{A_2}{2A_1} < \frac{KQ}{\alpha}$ and $A_2^2 - 4A_1A_3 = 0$, there exist three equilibria E_3^{II}, E_0 and E_{01}; the regular equilibrium E_3^{II} is a saddle-node, E_0 is an unstable node and the equilibrium E_{01} is a stable node.

Case C_3: When $\alpha > Q, \alpha\beta > 1, -\frac{A_2}{2A_1} \geq \frac{KQ}{\alpha}$ or $\alpha\beta \leq 1$, there exist two equilibria E_{01} and E_0; E_{01} is a stable node and E_0 is an unstable node.

Case D: $\alpha = Q$. In this case, we have two further scenarios to consider.

Case D_1: When $\alpha = Q, \alpha\beta > 1$ and $\alpha m_1 u < r_2(\alpha\beta - 1)$, there exist three equilibria E_5^{II}, E_0 and E_{01}; the regular equilibrium E_5^{II} is a stable node or focus, E_0 is an unstable node and the equilibrium E_{01} is a saddle.

Case D_2: When $\alpha = Q$ and $\alpha\beta > 1, \alpha m_1 u \geq r_2(\alpha\beta - 1)$ or $\alpha\beta \leq 1$, there exist two equilibria E_{01} and E_0; E_{01} is a stable node and E_0 is an unstable node.

3. Sliding dynamics

In this section, we will examine the dynamics on the hyperplane Σ, which lies along the boundary of adjacent regions. To this end, we initially investigate the existence of the sliding-mode region for Filippov system (3) and further analyse the dynamics of such a region. When the trajectories of the free subsystem and the control subsystem reach the sliding-mode region, new sliding dynamics will be generated in the sliding-mode region, and a class of new equilibria, which do not belong to the free-subsystem or the control-subsystem, will occur on the sliding-mode region. The total population of AC-Ds and AC-Is can then be theoretically contained at a predetermined threshold value.

3.1. Sliding-mode region of Filippov system (3)

In the previous section, we saw that Filippov system (3) consists of three parts: the free-subsystem, control-subsystem and the system defined exactly on the hyperplane Σ. The sliding-mode regions refer to the subregions of Σ with special properties; i.e., the vector fields of the free-subsystem and the control-subsystem on the sliding-mode region point towards each other. The sliding-mode region is defined as follows:

$$\Sigma_s = \left\{ Z \in \Sigma \middle| F_{G_1}(Z)\sigma(Z) \geq 0, F_{G_2}(Z)\sigma(Z) \leq 0 \right\}.$$

From the definition of the Lie derivative, we get that:

$$F_{G_1}(Z)\sigma(Z) = r_1\left(1 - \frac{X_1 + \alpha X_2}{K}\right)X_1 + r_2\left(1 - \frac{\beta X_1 + X_2}{K}\right)X_2$$

and

$$F_{G_2}(Z)\sigma(Z) = r_1(1-u)\left(1 - \frac{X_1 + \alpha X_2}{K}\right)X_1 + r_2\left(1 - \frac{\beta X_1 + X_2}{K}\right)X_2 - d_1uX_1.$$

When $F_{G_1}(Z)\sigma(Z) \geq 0$, we have

$$r_1\left(1 - \frac{X_1 + \alpha X_2}{K}\right)X_1 + r_2\left(1 - \frac{\beta X_1 + X_2}{K}\right)X_2 > 0.$$

On the sliding-mode region, we have $\sigma(Z) = X_1 + X_2 - ET = 0$. Substituting into the above inequality gives the following inequality with respect to X_1

$$\begin{aligned}&\Big(r_1(\alpha - 1) + r_2(\beta - 1)\Big)X_1^2 + \Big(r_1(K - \alpha ET) - r_2(K - ET) \\ &\quad + r_2(1-\beta)ET \Big) X_1 + r_2(K - ET)ET \geq 0.\end{aligned} \tag{7}$$

Denote

$$L_1(X_1) = l_{21}X_1^2 + l_{11}X_1 + l_{01},$$

where

$$l_{21} = r_1(\alpha - 1) + r_2(\beta - 1),$$
$$l_{11} = r_1(K - \alpha ET) - r_2(K - ET) + r_2(1-\beta)ET,$$
$$l_{01} = r_2(K - ET)ET.$$

It is natural to assume $ET < K$ due to the biological interpretation of K, which results in $l_{01} > 0$. If $L_1(X_1) = 0$, one can obtain two roots

$$X_1^u = \frac{-l_{11} - \sqrt{\Delta_1}}{2l_{21}}, \quad X_1^v = \frac{-l_{11} + \sqrt{\Delta_1}}{2l_{21}},$$

where $\Delta_1 = l_{11}^2 - 4l_{21}l_{01}$. For (7), we have the following three possibilities.

- If $l_{21} > 0$ and $l_{11} < 0$, we have $X_1^u \cdot X_1^v > 0$ and $X_1^u + X_1^v > 0$; the solution to (7) is $0 < X_1 \leq X_1^u$ or $X_1 \geq X_1^v$.
- If $l_{21} > 0$ and $l_{11} > 0$, we have $X_1^u \cdot X_1^v > 0$ and $X_1^u + X_1^v < 0$; solving (7) gives $X_1 > 0$.
- If $l_{21} < 0$, then (7) is true if and only if $0 < X_1 \leq X_1^u$.

When $F_{G_2}(Z)\sigma(Z) \leq 0$, we have

$$r_1(1-u)\left(1 - \frac{X_1 + \alpha X_2}{K}\right)X_1 + r_2\left(1 - \frac{\beta X_1 + X_2}{K}\right)X_2 - d_1uX_1 \leq 0.$$

Substituting $X_1 + X_2 - ET = 0$ into the above inequality, we have an inequality in X_1

$$l_{22}X_1^2 + l_{12}X_1 + l_{02} \leq 0, \tag{8}$$

where

$$l_{22} = r_1(1-u)(\alpha - 1) + r_2(\beta - 1), \qquad l_{02} = r_2(K - ET)ET,$$
$$l_{12} = r_1(1-u)(K - \alpha ET) - ud_1K + r_2(2ET - \beta ET - K).$$

Let $L_2(X_1) = l_{22}X_1^2 + l_{12}X_1 + l_{02}$. If $L_2(X_1) = 0$, we have two roots

$$X_1^m = \frac{-l_{12} - \sqrt{\Delta_2}}{2l_{22}}, \qquad X_1^n = \frac{-l_{12} + \sqrt{\Delta_2}}{2l_{22}},$$

where $\Delta_2 = l_{12}^2 - 4l_{22}l_{02}$. For (8), there are also three possibilities.

- If $l_{22} > 0, l_{12} < 0$, then X_1^m and X_1^n satisfy $X_1^m \cdot X_1^n > 0, X_1^m + X_1^n > 0$. Thus solving (8) yields $X_1^m \leq X_1 \leq X_1^n$.
- If $l_{22} > 0, l_{12} > 0$, then X_1^m and X_1^n satisfy $X_1^m \cdot X_1^n > 0, X_1^m + X_1^n < 0$. Thus inequality (8) is not satisfied for any X_1.
- If $l_{22} < 0$, we have $X_1^m \cdot X_1^n < 0$ and $L_2(X_1) \leq 0$ for $X_1 \geq X_1^m$.

According to all possible conditions that satisfy $L_1(X_1) \geq 0, L_2(X_1) \leq 0$ (i.e., $F_{G_1}(Z)\sigma(Z) \geq 0, F_{G_2}(Z)\sigma(Z) \leq 0$), we have the following six cases to describe the sliding-mode region of Filippov system (3).

Case H_1: $\alpha > 1, l_{21} > 0$ and $l_{11} < 0$. Denote

$$\Sigma_s^1 = \left\{ (X_1, X_2) \in R_+^2 \middle| \ X_1^m \leq X_1 \leq X_1^u, \ X_2 = ET - X_1 \right\},$$

$$\Sigma_s^2 = \left\{ (X_1, X_2) \in R_+^2 \middle| \ X_1^v \leq X_1 \leq X_1^n, \ X_2 = ET - X_1 \right\},$$

Table 2
Conditions for the occurrence of different sliding-mode regions.

Conditions			Sliding modes
Case H_1 $\alpha > 1, l_{21} > 0, l_{11} < 0$	$l_{22} > 0, l_{12} < 0$	$X_1^m < X_1^u, X_1^n < X_1^v$	Σ_s^1 or Σ_s^3
		$X_1^v < X_1^n, X_1^u < X_1^m$	Σ_s^2 or Σ_s^3
		$X_1^m < X_1^u, X_1^v < X_1^n$	$\Sigma_s^1 \cup \Sigma_s^2$
	$l_{22} < 0$	$X_1^u < X_1^m < X_1^v$	Σ_s^4
		$X_1^m < X_1^u$	$\Sigma_s^1 \cup \Sigma_s^4$
Case H_2 $\alpha > 1, l_{21} > 0, l_{11} > 0$	$l_{22} > 0, l_{12} < 0$		Σ_s^3
	$l_{22} < 0$		Σ_s^5
Case H_3 $\alpha > 1, l_{21} < 0$	$l_{22} < 0$	$X_1^m < X_1^u$	Σ_s^1
Case H_4 $\alpha < 1, l_{21} > 0, l_{11} < 0$	$l_{22} > 0, l_{12} < 0$		$\Sigma_s^1 \cup \Sigma_s^2$
Case H_5 $\alpha < 1,\ l_{21} > 0, l_{11} > 0$	$l_{22} > 0, l_{12} < 0$		Σ_s^3
Case H_6 $\alpha < 1, l_{21} < 0$	$l_{22} > 0, l_{12} < 0$	$X_1^m < X_1^u$	Σ_s^1 or Σ_s^3
	$l_{22} < 0$	$X_1^m < X_1^u$	Σ_s^1

$$\Sigma_s^3 = \left\{ (X_1, X_2) \in R_+^2 \middle| \ X_1^m \le X_1 \le X_1^n,\ X_2 = ET - X_1 \right\}.$$

If we further have $l_{22} > 0, l_{12} < 0$, the sliding-mode region Σ_s^1 or Σ_s^3 exists when $X_1^m < X_1^u$ and $X_1^n < X_1^v$ are satisfied; the sliding-mode region Σ_s^2 or Σ_s^3 exists when $X_1^v < X_1^n$ and $X_1^u < X_1^m$ are satisfied; if and only if both conditions $X_1^m < X_1^u$ and $X_1^v < X_1^n$ are satisfied, the sliding-mode region is $\Sigma_s^1 \bigcup \Sigma_s^2$.

Denote

$$\Sigma_s^4 = \left\{ (X_1, X_2) \in R_+^2 \middle| \ X_1 \ge X_1^v,\ X_2 = ET - X_1 \right\}.$$

If we further have $l_{22} < 0$, the sliding-mode region is Σ_s^4 when $X_1^u < X_1^m < X_1^v$ is satisfied, while the sliding-mode region is $\Sigma_s^1 \bigcup \Sigma_s^4$ when $X_1^m < X_1^u$ is satisfied.

Case H_2: $\alpha > 1$, $l_{21} > 0$ and $l_{11} > 0$. If we further have $l_{22} > 0, l_{12} < 0$, the sliding-mode region Σ_s^3 exists. If we have $l_{22} < 0$, the sliding-mode region Σ_s^5 exists, where

$$\Sigma_s^5 = \left\{ (X_1, X_2) \in R_+^2 \middle| \ X_1 \ge X_1^m,\ X_2 = ET - X_1 \right\}.$$

Case H_3: $\alpha > 1$ and $l_{21} < 0$. It is easy to get $l_{22} < 0$ since $l_{21} > l_{22}$ for $\alpha > 1$. The sliding-mode region Σ_s^1 exists when $X_1^m < X_1^u$.

Case H_4: $\alpha < 1$, $l_{21} > 0$ and $l_{11} < 0$. It is easy to get $l_{22} > 0$ since $l_{21} < l_{22}$ for $\alpha < 1$. In this case, we get $L_1(X_1) > L_2(X_1)$. If we further have $l_{12} < 0$, then the roots of $L_1(X_1) = 0$ and $L_2(X_2) = 0$ satisfy $X_1^m < X_1^u < X_1^v < X_1^n$, so the sliding-mode region takes the form $\Sigma_s^1 \bigcup \Sigma_s^2$. If we have $l_{12} > 0$, no sliding-mode region exists.

Case H_5: $\alpha < 1$, $l_{21} > 0$ and $l_{11} > 0$. In this case, we similarly have $l_{22} > 0$ since $l_{21} < l_{22}$ for $\alpha < 1$. If we further have $l_{12} < 0$, the sliding-mode region is Σ_s^3. If we have $l_{12} > 0$, no sliding-mode region exists.

Case H_6: $\alpha < 1$ and $l_{21} < 0$. If we further have $l_{22} > 0, l_{12} < 0$, the sliding-mode region Σ_s^1 or Σ_s^3 exists when $X_1^m < X_1^u$ is satisfied. If we have $l_{22} < 0$, the sliding-mode region Σ_s^1 exists when $X_1^m < X_1^u$ is satisfied.

We summarize all conditions in which sliding-mode regions may occur in Table 2.

3.2. Sliding dynamics of Filippov system (3)

From the above discussion, we can get that the sliding-mode regions are different under different parameters. Further, we will examine the sliding dynamics of Filippov system (3). Generally, there are three methods to solve the dynamics of system (3) on the sliding-mode region: the Filippov convex method, Utkin's equivalent control method and the singular perturbation method. In the following, we will employ the Filippov convex method to determine the sliding-mode dynamics of Filippov system (3).

Denote any sliding-mode region as Σ_s. It follows from Section 2 that the sliding-mode dynamics of Filippov system (3) are determined by (4), where Σ_s is given in Table 2. Since $\hat{F}(Z)$ is tangent to the sliding-mode region Σ_s, one can obtain that $\hat{F}(Z)\sigma(Z) = 0$ on the sliding-mode region. It follows that

$$qF_{11}(Z) + (1-q)F_{21}(Z) + qF_{12}(Z) + (1-q)F_{22}(Z) = 0.$$

Solving with respect to q gives

$$q = \frac{F_{21}(Z) + F_{22}(Z)}{F_{21}(Z) - F_{11}(Z) + F_{22}(Z) - F_{12}(Z)}. \tag{9}$$

Substituting (9) into (4), we derive the sliding dynamics of the Filippov system (3) as follows

$$\begin{aligned} \frac{\mathrm{d}X_1}{\mathrm{d}t} &= qF_{11}(Z) + (1-q)F_{21}(Z) = \frac{\Gamma_1}{\Gamma_2}, \\ \frac{\mathrm{d}X_2}{\mathrm{d}t} &= qF_{12}(Z) + (1-q)F_{22}(Z) = -\frac{\Gamma_1}{\Gamma_2}, \end{aligned} \tag{10}$$

where

$$\begin{aligned} \Gamma_1 &= F_{22}(Z)F_{11}(Z) - F_{21}(Z)F_{12}(Z) \\ &= r_1 X_1 \left(1 - \frac{X_1 + \alpha X_2}{K}\right) \left[r_2 \left(1 - \frac{\beta X_1 + X_2}{K}\right) X_2 + u m_1 X_1 \right] \\ &\quad - r_2 X_2 \left(1 - \frac{\beta X_1 + X_2}{K}\right) \left[r_1 (1-u) X_1 \left(1 - \frac{X_1 + \alpha X_2}{K}\right) \right. \\ &\quad \left. - (d_1 + m_1) u X_1 \right], \\ \Gamma_2 &= F_{21}(Z) - F_{11}(Z) + F_{22}(Z) - F_{12}(Z) = -r_1 u X_1 \left(1 - \frac{X_1 + \alpha X_2}{K}\right) \\ &\quad - u d_1 X_1. \end{aligned} \tag{11}$$

Since on the sliding-mode region Σ_s, we have $X_1 + X_2 = ET$, direct calculation yields that $\frac{dX_1}{dt} = -\frac{dX_2}{dt}$, which can also be derived from (10). Therefore, we only focus on the dynamics of

$$\frac{dX_1}{dt} = \frac{\Gamma_1}{\Gamma_2}. \tag{12}$$

We next examine the existence of the equilibria on the sliding mode Σ_s; i.e., the pseudo-equilibria of Filippov system (3). To this end, we need to compute all possible nonnegative equilibria of (12), which is equivalent to $\Gamma_1 = 0$. Let

$$\gamma_3 = r_1 r_2 u(\alpha-1)(\beta-1),$$
$$\gamma_2 = r_1 r_2 u(3\alpha - 2\alpha\beta + \beta - 2)ET + r_1 r_2 u(\beta-\alpha)K + r_2 uK(d_1+m_1)(\beta-1) + r_1 m_1 uK(\alpha-1),$$
$$\gamma_1 = r_1 r_2 u(\alpha\beta + 1 - 3\alpha)ET^2 + \Big[r_1 r_2 uK(2\alpha - \beta + 1) + r_2 uK(d_1+m_1)(2-\beta) - \alpha r_1 m_1 uK \Big] ET - r_1 r_2 uK^2 - r_2 u(d_1+m_1)K^2 + r_1 m_1 uK^2,$$
$$\gamma_0 = (K-ET)ET\Big[r_1 r_2 u(K-\alpha ET) + r_2 u(d_1+m_1)K\Big].$$

Substituting $X_1 + X_2 = ET$ into $\Gamma_1 = 0$ is equivalent to the following equations with respect to X_1

$$\Gamma(X_1) \equiv \gamma_3 X_1^3 + \gamma_2 X_1^2 + \gamma_1 X_1 + \gamma_0 = 0. \tag{13}$$

For convenience, we rewrite γ_1, γ_2 as

$$\gamma_1 = \gamma_{12} ET^2 + \gamma_{11} ET + \gamma_{10}, \quad \gamma_2 = \gamma_{21} ET + \gamma_{20},$$

where

$$\gamma_{12} = r_1 r_2 u(\alpha\beta - 3\alpha + 1),$$
$$\gamma_{11} = r_1 r_2 uK(2\alpha - \beta + 1) + r_2 uK(d_1+m_1)(2-\beta) - \alpha r_1 m_1 uK,$$
$$\gamma_{10} = -r_1 r_2 uK^2 - r_2 u(d_1+m_1)K^2 + r_1 m_1 uK^2,$$
$$\gamma_{21} = r_1 r_2 u(3\alpha - 2\alpha\beta + \beta - 2),$$
$$\gamma_{20} = r_1 r_2 u(\beta-\alpha)K + r_2 uK(d_1+m_1)(\beta-1) + r_1 m_1 uK(\alpha-1).$$

There are at most three roots for $\Gamma(X_1)$, which we denote as X_1^a, X_1^b and X_1^c. According to Vieta's theorem, we have

$$X_1^a + X_1^b + X_1^c = -\frac{\gamma_2}{\gamma_3}, \qquad X_1^a \cdot X_1^b \cdot X_1^c = -\frac{\gamma_0}{\gamma_3}. \tag{14}$$

Let $X_1 = y - \frac{\gamma_2}{3\gamma_3}$ and divide both sides of (13) by γ_3, so that (13) can be rewritten as

$$y^3 + n_1 y + n_0 = 0, \tag{15}$$

where

$$n_1 = \frac{\gamma_1}{\gamma_3} - \frac{\gamma_2^2}{3\gamma_3^2}, \qquad n_0 = \frac{\gamma_0}{\gamma_3} + \frac{2\gamma_2^3}{27\gamma_3^3} - \frac{\gamma_1\gamma_2}{3\gamma_3^2}.$$

Denote $N = \left(\frac{n_1}{3}\right)^3 + \left(\frac{n_0}{2}\right)^2$. By using Cardano's formula and the relationship between Eqs. (13) and (15), we have the following three cases:

- If $N < 0$, there are three distinct real roots for $\Gamma(X_1)$.
- If $N = 0$, there is one real root of multiple three or two distinct real roots with one of them being multiple two for $\Gamma(X_1)$.
- If $N > 0$, there exists one real root and a pair of conjugate complex roots for $\Gamma(X_1)$.

In order to verify the existence of pseudo-equilibria, we analyse the sign of each real root by using Vieta's theorem. There are three possibilities to consider: $\gamma_0 > 0, \gamma_0 < 0$ and $\gamma_0 = 0$. We initially consider the first possibility $\gamma_0 > 0$, which is equivalent to $K - \alpha ET > -\frac{r_2(d_1+m_1)K}{r_1 r_2}$, and we have three further cases to discuss.

Case Q_1: $\gamma_0 > 0, N < 0$. In this case, there exist three roots X_1^a, X_1^b and X_1^c for (13), and we next examine the existence of positive real roots. There are four further possibilities to consider depending on the sign of γ_2 and γ_3.

Case Q_1^1: $\gamma_2 > 0, \gamma_3 > 0$. It is easy to derive $X_1^a + X_1^b + X_1^c < 0$, $X_1^a \cdot X_1^b \cdot X_1^c < 0$ in this scenario. It follows that there is one negative root and two positive roots (shown in as shown in Fig. 1(a)) or three negative roots (shown in Fig. 1(b)). Direct calculation yields $\gamma_3 > 0$ if

$$\alpha < 1, \beta < 1$$

or

$$\alpha > 1, \beta > 1.$$

To ensure $\gamma_2 > 0$, it is necessary to discuss the sign of γ_{21} and γ_{20}. We get $\gamma_2 > 0$ if one of the following conditions holds:

- $\gamma_{21} > 0, \gamma_{20} > 0$;
- $\gamma_{21} > 0, \gamma_{20} < 0, ET > -\frac{\gamma_{20}}{\gamma_{21}}$;
- $\gamma_{21} < 0, \gamma_{20} > 0, 0 < ET < -\frac{\gamma_{20}}{\gamma_{21}}$.

Table 3
Conditions for the existence of two positive roots in Case Q_1^1.

$\gamma_0 > 0, N < 0$	$\alpha < 1, \beta < 1, \gamma_1 < 0$	$\gamma_{21} > 0, \gamma_{20} > 0$	for all ET
		$\gamma_{21} > 0, \gamma_{20} < 0$	$ET > -\frac{\gamma_{20}}{\gamma_{21}}$
		$\gamma_{21} < 0, \gamma_{20} > 0$	$0 < ET < -\frac{\gamma_{20}}{\gamma_{21}}$
	$\alpha > 1, \beta > 1, \gamma_1 < 0$	$\gamma_{21} > 0, \gamma_{20} > 0$	for all ET
		$\gamma_{21} > 0, \gamma_{20} < 0$	$ET > -\frac{\gamma_{20}}{\gamma_{21}}$
		$\gamma_{21} < 0, \gamma_{20} > 0$	$0 < ET < -\frac{\gamma_{20}}{\gamma_{21}}$

Concluding the above discussions, we obtain that there exist two positive roots and one negative root or three negative roots for (13) if one of the following conditions is true:

- $\alpha < 1, \beta < 1, \gamma_{21} > 0, \gamma_{20} > 0$;
- $\alpha < 1, \beta < 1, \gamma_{21} > 0, \gamma_{20} < 0, ET > -\frac{\gamma_{20}}{\gamma_{21}}$;
- $\alpha < 1, \beta < 1, \gamma_{21} < 0, \gamma_{20} > 0, 0 < ET < -\frac{\gamma_{20}}{\gamma_{21}}$;
- $\alpha > 1, \beta > 1, \gamma_{21} > 0, \gamma_{20} > 0$;
- $\alpha > 1, \beta > 1, \gamma_{21} > 0, \gamma_{20} < 0, ET > -\frac{\gamma_{20}}{\gamma_{21}}$;
- $\alpha > 1, \beta > 1, \gamma_{21} < 0, \gamma_{20} > 0, 0 < ET < -\frac{\gamma_{20}}{\gamma_{21}}$.

Differentiating $\Gamma(X_1)$ with respect to X_1 gives

$$\Gamma'(X_1) = 3\gamma_3 X_1^2 + 2\gamma_2 X_1 + \gamma_1.$$

Solving $\Gamma'(X_1) = 0$ with respect to X_1 yields two roots, the larger of which is

$$X'_{11} = \frac{-\gamma_2 + \sqrt{\gamma_2^2 - 3\gamma_3\gamma_1}}{3\gamma_3}. \tag{16}$$

If $X'_{11} > 0$, there are two positive roots and one negative root for (13), as shown in Fig. 1. In fact, we have $X'_{11} > 0$ if $\gamma_3 > 0$ and $\gamma_1 < 0$. Thus the conditions for the existence of two positive roots (X_1^b, X_1^c), can be obtained. For convenience, we denote the conditions $(N < 0, \gamma_0 > 0, \gamma_1 < 0, \gamma_3 > 0, \gamma_2 > 0)$ to guarantee two positive roots in this case as Q_1^{11} below. The detailed conditions for the two positive roots are summarized in Table 3.

Case Q_1^2: $\gamma_3 > 0$ and $\gamma_2 \le 0$. In this case, we have $X_1^a + X_1^b + X_1^c \ge 0$ and $X_1^a \cdot X_1^b \cdot X_1^c < 0$, so there exists one negative root (X_1^a, shown in Fig. 1(a)) and two positive roots (X_1^b and X_1^c, shown in Fig. 1(a)). We similarly get $\gamma_2 \le 0$ if one of the following conditions is true:

- $\gamma_{21} > 0, \gamma_{20} < 0, 0 < ET < -\frac{\gamma_{20}}{\gamma_{21}}$;
- $\gamma_{21} < 0, \gamma_{20} < 0$;
- $\gamma_{21} < 0, \gamma_{20} > 0, ET > -\frac{\gamma_{20}}{\gamma_{21}}$;
- $ET = -\frac{\gamma_{20}}{\gamma_{21}}$.

Similarly, we derive the conditions to guarantee the existence of exactly two positive roots and summarize them in Table 4.

Case Q_1^3: $\gamma_3 < 0$ and $\gamma_2 \le 0$. In this case, we have $X_1^a + X_1^b + X_1^c \le 0$ and $X_1^a \cdot X_1^b \cdot X_1^c > 0$, so there exist one positive root (X_1^a, shown in Fig. 2(a)) and two negative roots (X_1^c and X_1^b, shown in Fig. 2(a)). We obtain the conditions for the existence of exactly one positive root and summarize them in Table 5.

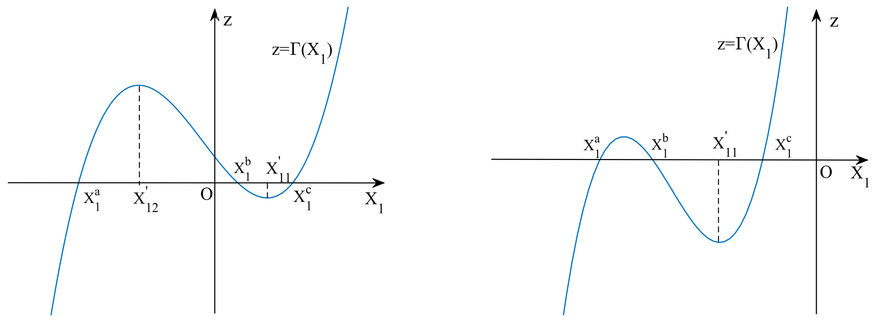

(a) (b)

Fig. 1. Schematic diagram to show the potential arrangement of the roots of (13) in Cases Q_1^1 and Q_1^2.

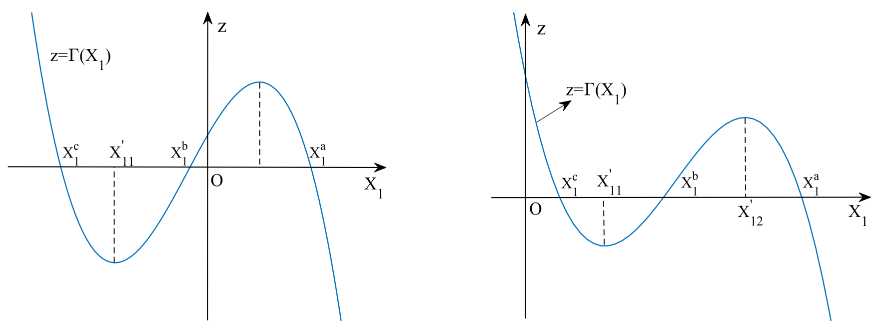

(a) (b)

Fig. 2. Schematic diagram to show the potential arrangement of the roots of (13) in Cases Q_1^3 and Q_1^4.

Table 4
Conditions for the existence of two positive roots in Case Q_1^2.

$\gamma_0 > 0, N < 0$	$\alpha < 1, \beta < 1$	$\gamma_{21} > 0, \gamma_{20} < 0$	$0 < ET < -\frac{\gamma_{20}}{\gamma_{21}}$
		$\gamma_{21} < 0, \gamma_{20} < 0$	for all ET
		$\gamma_{21} < 0, \gamma_{20} > 0$	$ET > -\frac{\gamma_{20}}{\gamma_{21}}$
		$\gamma_2 = 0$	$ET = -\frac{\gamma_{20}}{\gamma_{21}}$
	$\alpha > 1, \beta > 1$	$\gamma_{21} > 0, \gamma_{20} < 0$	$0 < ET < -\frac{\gamma_{20}}{\gamma_{21}}$
		$\gamma_{21} < 0, \gamma_{20} < 0$	for all ET
		$\gamma_{21} < 0, \gamma_{20} > 0$	$ET > -\frac{\gamma_{20}}{\gamma_{21}}$
		$\gamma_2 = 0$	$ET = -\frac{\gamma_{20}}{\gamma_{21}}$

Table 5
Conditions for the existence of one positive root in Case Q_1^3.

$\gamma_0 > 0, N < 0$	$\alpha > 1, \beta < 1$	$\gamma_{21} > 0, \gamma_{20} < 0$	$0 < ET < -\frac{\gamma_{20}}{\gamma_{21}}$
		$\gamma_{21} < 0, \gamma_{20} < 0$	for all ET
		$\gamma_{21} < 0, \gamma_{20} > 0$	$ET > -\frac{\gamma_{20}}{\gamma_{21}}$
		$\gamma_2 = 0$	$ET = -\frac{\gamma_{20}}{\gamma_{21}}$
	$\alpha < 1, \beta > 1$	$\gamma_{21} > 0, \gamma_{20} < 0$	$0 < ET < -\frac{\gamma_{20}}{\gamma_{21}}$
		$\gamma_{21} < 0, \gamma_{20} < 0$	for all ET
		$\gamma_{21} < 0, \gamma_{20} > 0$	$ET > -\frac{\gamma_{20}}{\gamma_{21}}$
		$\gamma_2 = 0$	$ET = -\frac{\gamma_{20}}{\gamma_{21}}$

Case Q_1^4: $\gamma_3 < 0$ and $\gamma_2 > 0$. In this case, we have $X_1^a + X_1^b + X_1^c > 0$ and $X_1^a \cdot X_1^b \cdot X_1^c > 0$, so there is one positive root (X_1^a, shown in Fig. 2(a)) and two negative roots (X_1^c and X_1^b, shown in Fig. 2(a)) or three positive roots (X_1^a, X_1^b and X_1^c, shown in Fig. 2(b)). Whether there is only one positive root or three positive roots in this scenario depends on the sign of the smaller root X'_{11} of $\Gamma'(X_1) = 0$, where X'_{11} is defined as in formula (16). If $X'_{11} > 0$, there are three positive roots, as shown in Fig. 2(b). Otherwise, there is only one positive root. Direct calculation yields that $X'_{11} > 0$ for $\gamma_3 < 0, \gamma_1 < 0$ and $X'_{11} < 0$ for $\gamma_3 < 0, \gamma_1 > 0$. Similarly, we can derive the conditions for the existence of three positive roots or one positive root. For convenience, we denote the conditions ($N < 0, \gamma_0 > 0, \gamma_1 > 0, \gamma_3 < 0, \gamma_2 > 0$) guaranteeing one positive root as Q_1^{41}, while the conditions ($N < 0, \gamma_0 > 0, \gamma_1 < 0, \gamma_3 < 0, \gamma_2 > 0$) guaranteeing three positive root are denoted as Q_1^{42}. The detailed conditions for one or three positive roots are summarized in Table 6.

Case Q_2: When $N = 0$, there are three real roots for $\Gamma(X_1) = 0$. If we further have $n_1 \neq 0, n_0 \neq 0$, there is a real root of multiplicity two and a single real root (shown in Fig. 3(a),(b),(d),(e)); otherwise, we have a real root of multiplicity three (shown in Fig. 3(c)). It is sufficient to examine the existence of positive real roots for (13), as shown in Fig. 3. In Fig. 3(a), X_1^c is the single positive real root and X_1^A is the positive real root of multiplicity two. The single positive real root and positive real root of multiplicity two are X_1^a and X_1^B in Fig. 3(b), respectively. Only one single positive real root X_1^a exists for (13) in Fig. 3(d), while a positive real root of multiplicity two (X_1^A) exists for (13) in Fig. 3(e). In Fig. 3(c), X_1^D is the real root of multiplicity three. Similar to Case Q_1, we can obtain the conditions ($N = 0, \gamma_0 > 0, n_1 \neq 0, n_0 \neq 0, \gamma_1 < 0, \gamma_3 < 0, \gamma_2 > 0$) for the existence of two distinct positive real roots, as shown in Fig. 3(a) and (b). For convenience, we denote the conditions as Q_2^1 below. By replacing $n_1 \neq 0, n_0 \neq 0$ with $n_1 = 0, n_0 = 0$, we obtain the conditions that Eq. (13) has one positive real root of multiplicity three, as shown in Fig. 3(c). We similarly denote this set of conditions as Q_2^2 in the following. We can get only one positive root X_1^a for (13) if $N = 0, \gamma_0 > 0, n_1 \neq 0, n_0 \neq 0, \gamma_1 < 0, \gamma_3 > 0, \gamma_2 > 0$, which we denote as Q_2^3 below, are true. There exists one positive root X_1^A of multiplicity two if $N = 0, \gamma_0 > 0, n_1 \neq 0, n_0 \neq 0, \gamma_1 > 0, \gamma_3 < 0, \gamma_2 > 0$, which we

Table 6
Conditions for the existence of positive roots for Case Q_1^4.

Conditions			Number of positive roots
$\gamma_0 > 0, N < 0$	$\alpha > 1, \beta < 1, \gamma_1 < 0$	$\gamma_{21} > 0, \gamma_{20} < 0, ET > -\frac{\gamma_{20}}{\gamma_{21}}$ $\gamma_{21} > 0, \gamma_{20} > 0$, for all ET $\gamma_{21} < 0, \gamma_{20} > 0, 0 < ET < -\frac{\gamma_{20}}{\gamma_{21}}$	Three
	$\alpha < 1, \beta > 1, \gamma_1 < 0$	$\gamma_{21} > 0, \gamma_{20} < 0, ET > -\frac{\gamma_{20}}{\gamma_{21}}$ $\gamma_{21} > 0, \gamma_{20} > 0$, for all ET $\gamma_{21} < 0, \gamma_{20} > 0, 0 < ET < -\frac{\gamma_{20}}{\gamma_{21}}$	
	$\alpha > 1, \beta < 1, \gamma_1 > 0$	$\gamma_{21} > 0, \gamma_{20} < 0, ET > -\frac{\gamma_{20}}{\gamma_{21}}$ $\gamma_{21} > 0, \gamma_{20} > 0$, for all ET $\gamma_{21} < 0, \gamma_{20} > 0, 0 < ET < -\frac{\gamma_{20}}{\gamma_{21}}$	One
	$\alpha < 1, \beta > 1, \gamma_1 > 0$	$\gamma_{21} > 0, \gamma_{20} < 0, ET > -\frac{\gamma_{20}}{\gamma_{21}}$ $\gamma_{21} > 0, \gamma_{20} > 0$, for all ET $\gamma_{21} < 0, \gamma_{20} > 0, 0 < ET < -\frac{\gamma_{20}}{\gamma_{21}}$	

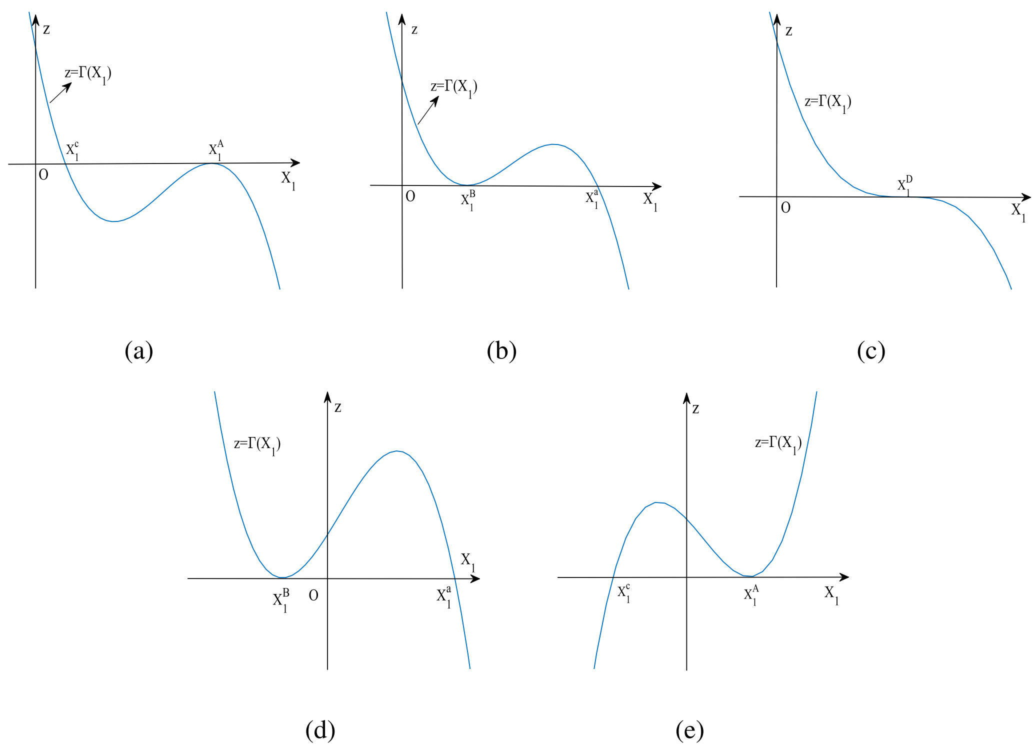

Fig. 3. Possible roots of $\Gamma(X_1) = 0$ for Case Q_2.

Table 7
Conditions for the existence of two distinct real roots for Case Q_2.

$\gamma_0 > 0, N = 0, n_1 \neq 0, n_0 \neq 0$	$\alpha > 1, \beta < 1, \gamma_1 < 0$	$\gamma_{21} > 0, \gamma_{20} < 0, ET > -\frac{\gamma_{20}}{\gamma_{21}}$ $\gamma_{21} > 0, \gamma_{20} > 0$, for all ET $\gamma_{21} < 0, \gamma_{20} > 0, 0 < ET < -\frac{\gamma_{20}}{\gamma_{21}}$
	$\alpha < 1, \beta > 1, \gamma_1 < 0$	$\gamma_{21} > 0, \gamma_{20} < 0, ET > -\frac{\gamma_{20}}{\gamma_{21}}$ $\gamma_{21} > 0, \gamma_{20} > 0$, for all ET $\gamma_{21} < 0, \gamma_{20} > 0, 0 < ET < -\frac{\gamma_{20}}{\gamma_{21}}$

denote as Q_2^4 below. We listed the detailed conditions to guarantee the existence of two positive real roots in this case in Table 7.

Case Q_3: When $N > 0$, there is one real root and two conjugate complex roots for $\Gamma(X_1) = 0$, as shown in Fig. 4. Since the product of two conjugate complex roots is positive, there is one positive real root for Eq. (13) if $\gamma_3 < 0$ according to (14). Further discussion yields that $\gamma_3 < 0$ if and only if $\alpha > 1, \beta < 1$ or $\alpha < 1, \beta > 1$.

From the positive real root of Eq. (13), we derive the possible pseudo-equilibria for the sliding-mode dynamics (12). Denote all the (boundary) pseudo-equilibria by $E_s^z = (X_1^z, X_2^z), z \in \{a, b, c, A, B, D\}$, where X_1^z is defined as above and $X_2^z = ET - X_1^z$. The existence of all possible pseudo-equilibria has thus been examined above. If the possible pseudo-equilibrium $E_s^z, z \in \{a, b, c, A, B, D\}$ lies on the sliding-mode region (i.e., $E_s^z \in \Sigma_s$), then it is a pseudo-equilibrium of Filippov system (3). If $E_s^z, z \in \{a, b, c, A, B, D\}$ is a pseudo-equilibria of Filippov system (3), the stability can be analysed by examining the sign of Eq. (12) at any point $(X_1, X_2) \in U(E_s^z)$, where $U(E_s^z)$ is some neighbourhood of E_s^z. Since $\Gamma_2 < 0$ for any $X_1, X_2 < ET$, we get that

$$\operatorname{sgn}\left\{ \frac{\mathrm{d}X_1}{\mathrm{d}t}\Big|_{(X_1,X_2)} \right\} = \operatorname{sgn}\Big\{ -\Gamma(X_1) \Big\}$$

for any $(X_1, X_2) \in U(E_s^z)$. For the pseudo-equilibrium E_s^b in case Q_1^{11}, it follows from the discussion in Q_1^{11} and Fig. 1 that $\Gamma(X_1) > 0$ for $X_1 \in U(X_1^b)$ and $X_1 < X_1^b$ while $\Gamma(X_1) < 0$ for $X_1 \in U(X_1^b)$ and $X_1 > X_1^b$, so E_s^b is unstable. Similarly, we get that the pseudo-equilibrium E_s^a is unstable in Cases Q_1^3, Q_1^{41}, Q_2^1, Q_2^3, Q_1^{42} and Q_3; the pseudo-equilibrium E_s^b in Case Q_1^2 is unstable, but it is stable in Case Q_1^{42}; the pseudo-equilibrium E_s^c is stable in Cases Q_1^{11} and Q_1^2 but it is unstable in Cases

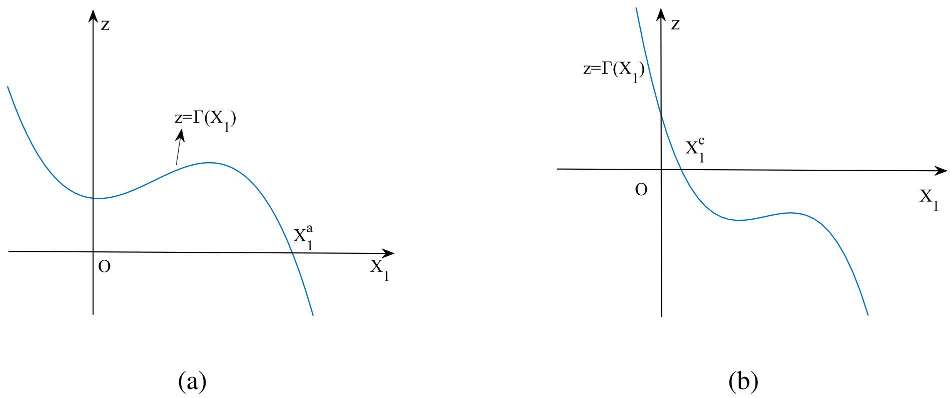

Fig. 4. The roots of $\Gamma(X_1) = 0$ for Case Q_3.

Table 8
Conditions for the existence of different pseudo-equilibria and their stability. In the penultimate row, the parentheses refer to the two possibilities for a single pseudo-equilibrium and a pseudo-equilibrium of multiplicity two in Fig. 3(b), as distinct from Fig. 3(a).

Number of pseudo-equilibria	Conditions		Pseudo-equilibria and their stability
One	$N < 0, \gamma_0 > 0, \gamma_3 < 0, \gamma_2 \le 0$ $N < 0, \gamma_0 > 0, \gamma_1 > 0, \gamma_3 < 0, \gamma_2 > 0$ $N = 0, \gamma_0 > 0, n_1 \ne 0, n_0 \ne 0, \gamma_1 < 0, \gamma_3 > 0, \gamma_2 > 0$	Q_1^3 Q_1^{41} Q_2^3	E_s^{au}
	$N > 0, \gamma_0 > 0, \gamma_3 < 0$	Q_3	E_s^{au} or E_s^{cu}
	$N = 0, \gamma_0 > 0, n_1 \ne 0, n_0 \ne 0, \gamma_1 > 0, \gamma_3 < 0, \gamma_2 > 0$	Q_2^4	E_s^{Au}
	$N = 0, \gamma_0 > 0, n_1 = 0, n_0 = 0, \gamma_1 < 0, \gamma_3 < 0, \gamma_2 > 0$	Q_2^2	E_s^{Du}
Two	$N < 0, \gamma_0 > 0, \gamma_1 < 0, \gamma_3 > 0, \gamma_2 > 0$ $N < 0, \gamma_0 > 0, \gamma_3 > 0, \gamma_2 \le 0$	Q_1^{11} Q_1^2	E_s^{bu}, E_s^{cs}
	$N = 0, \gamma_0 > 0, n_1 \ne 0, n_0 \ne 0, \gamma_1 < 0, \gamma_3 < 0, \gamma_2 > 0$	Q_2^1	E_s^{Au} (E_s^{Bu}), E_s^{cu} (E_s^{au})
Three	$N < 0, \gamma_0 > 0, \gamma_1 < 0, \gamma_3 < 0, \gamma_2 > 0$	Q_1^{42}	$E_s^{au}, E_s^{bs}, E_s^{cu}$

Q_1^{42}, Q_2^1 and Q_3; the pseudo-equilibria E_s^A, E_s^B and E_s^D in Cases Q_2^1 and Q_2^2 are unstable. Concluding the above discussion, we get the following result.

Theorem 1. *When $\gamma_0 > 0$, the sliding dynamics of Filippov system (3) are as follows.*

(i) There exists one unstable pseudo-equilibrium if one of the conditions $Q_1^3, Q_1^{41}, Q_2^3, Q_3, Q_2^4, Q_2^2$ holds.

(ii) Two pseudo-equilibria exist if the condition Q_1^{11} or Q_1^2 holds, one of which is stable and the other one is unstable; conversely, two unstable pseudo-equilibria exist if the condition Q_2^1 holds.

(iii) Three pseudo-equilibria exist if the condition Q_1^{42} holds and one of them is stable.

For clarity, we have listed the conditions for the existence of all pseudo-equilibria and the stability of each pseudo-equilibrium in Table 8. In Table 8, the superscript 's' of the pseudo-equilibrium E_s^z represents stable and the superscript 'u' represents unstable. For instance, E_s^{as} demonstrates that E_s^a is stable and E_s^{au} demonstrates that E_s^a is unstable.

Next, we examine the existence of all possible pseudo-equilibria and their stability for $\gamma_0 < 0$ by implementing a similar analysis for the case $\gamma_0 > 0$. The details are given in Appendix A. It follows from this appendix that there are a total of six possible positive real roots ($X_1^a, X_1^b, X_1^c, X_1^A, X_1^B$ and X_1^D) for (15). Thus we can get all possible pseudo-equilibria $E_s^a, E_s^b, E_s^c, E_s^A, E_s^B$ and E_s^D for the sliding-mode dynamics (3). If the pseudo-equilibrium $E_s^z, z \in \{a, b, c, A, B, D\}$ lie on the sliding-mode region Σ_s, the stability can be analysed. Here we omit the details and summarize the conditions for the existence of all pseudo-equilibria and the stability of each pseudo-equilibrium in the following theorem.

Theorem 2. *When $\gamma_0 < 0$, the sliding dynamics of Filippov system (3) is as follows.*

(i) There is a stable pseudo-equilibrium if one of the conditions $P_1^1, P_1^{21}, P_3, P_2^3, P_2^4$ or P_2^2 hold, whereas an unstable pseudo-equilibrium exists if the condition P_2^5 or P_2^6 holds.

(ii) There are two pseudo-equilibria if one of the conditions P_1^{31}, P_1^4 or P_2^1 hold. One is stable, and the other is unstable.

(iii) Three pseudo-equilibria exist, two of which are stable if the condition P_1^{22} holds.

For clarity, we list the conditions for the existence of all pseudo-equilibria and the stability of each pseudo-equilibrium in Table 9. It follows from Table 9 that the pseudo-equilibrium E_s^a is unstable in Cases P_1^{31} and P_1^4, and it is stable in Cases P_1^{22} and P_2^1; the pseudo-equilibrium E_s^b is stable in Cases P_1^{31} and P_1^4, and it is unstable in Case P_1^{22}; E_s^c is stable in Cases $P_1^1, P_1^{21}, P_1^{22}, P_2^1, P_2^3, P_2^4$ and P_3; E_s^A and E_s^B are unstable in Cases P_2^1, P_2^5 and P_2^6; E_s^D is stable in Case P_2^2.

Next, we examine the existence of pseudo-equilibria for the Filippov system (3) when $\gamma_0 = 0$; i.e., $K - \alpha ET = \frac{(d_1+m_1)K}{r_1}$ or $K = ET$. See Appendix B for the details. It follows from this appendix that there are four possible pseudo-equilibria $E_s^z = (X_1^z, X_2^z)$, where $X_2^z = ET - X_1^z$ and $z \in \{e, f, E, F\}$. We summarize the results in Theorem 3 and omit the details here.

Theorem 3. *When $\gamma_0 = 0$, the sliding dynamics of Filippov system (3) are as follows.*

(i) There is one stable pseudo-equilibrium if one of the conditions M_1^1, M_2^2 or M_5^2 hold, whereas there is one unstable pseudo-equilibrium if one of the conditions M_3^1, M_4^1, M_5^1 or M_6^1 hold.

(ii) There are two pseudo-equilibria, and one of them is stable, if one of M_2^1 or M_3^2 holds.

Table 9
Conditions for the existence of all pseudo-equilibria and their stability.

Number of pseudo-equilibria	Conditions		Pseudo-equilibria and their stability
One	$N<0,\gamma_0<0,\gamma_3>0,\gamma_2\geq 0$	P_1^1	E_s^{cs}
	$N<0,\gamma_0<0,\gamma_1<0,\gamma_3>0,\gamma_2<0$	P_1^{21}	
	$N>0,\gamma_0<0,\gamma_3>0$	P_3	
	$N=0,\gamma_0<0,n_1\neq 0,n_0\neq 0,\gamma_3>0,\gamma_2\geq 0$	P_2^3	
	$N=0,\gamma_0<0,n_1\neq 0,n_0\neq 0,\gamma_1<0,\gamma_3>0,\gamma_2<0$	P_2^4	
	$N=0,\gamma_0<0,n_1\neq 0,n_0\neq 0,\gamma_3<0,\gamma_2<0$	P_2^5	E_s^{Au}
	$N=0,\gamma_0<0,n_1\neq 0,n_0\neq 0,\gamma_1<0,\gamma_3<0,\gamma_2\geq 0$	P_2^6	
	$N=0,\gamma_0<0,n_1=0,n_0=0,\gamma_1>0,\gamma_3>0,\gamma_2<0$	P_2^2	E_s^{Ds}
Two	$N<0,\gamma_0<0,\gamma_1>0,\gamma_3<0,\gamma_2<0$	P_1^{31}	E_s^{au}, E_s^{bs}
	$N<0,\gamma_0<0,\gamma_3<0,\gamma_2\geq 0$	P_1^4	
	$N=0,\gamma_0<0,n_1\neq 0,n_0\neq 0,\gamma_1>0,\gamma_3>0,\gamma_2<0$	P_2^1	E_s^{Au} (E_s^{Bu}), E_s^{cs} (E_s^{as})
Three	$N<0,\gamma_0<0,\gamma_1>0,\gamma_3>0,\gamma_2<0$	P_1^{22}	$E_s^{as}, E_s^{bu}, E_s^{cs}$

Table 10
Conditions for the existence of different pseudo-equilibria and their stabilities when $\gamma_0=0$.

Number of pseudo-equilibria	Conditions		Pseudo-equilibria and their stability
One	$\Omega_0>0,\gamma_3>0,\gamma_2>0,\gamma_1<0$	M_1^1	E_s^{fs}
	$\Omega_0>0,\gamma_3>0,\gamma_2<0,\gamma_1<0$	M_2^2	
	$\Omega_0>0,\gamma_3<0,\gamma_2>0,\gamma_1>0$	M_3^1	E_s^{eu}
	$\Omega_0>0,\gamma_3<0,\gamma_2<0,\gamma_1>0$	M_4^1	
	$\Omega_0>0,\gamma_3<0,\gamma_2=0,\gamma_1>0$	M_5^1	E_s^{Eu}
	$\Omega_0>0,\gamma_3>0,\gamma_2=0,\gamma_1<0$	M_5^2	E_s^{Es}
	$\Omega_0=0,\gamma_3\cdot\gamma_2<0$	M_6^1	E_s^{Fu}
Two	$\Omega_0>0,\gamma_3>0,\gamma_2<0,\gamma_1>0$	M_2^1	E_s^{eu}, E_s^{fs}
	$\Omega_0>0,\gamma_3<0,\gamma_2>0,\gamma_1<0$	M_3^2	

For clarity, we summarize the conditions for the existence of all pseudo-equilibria and the stability of each pseudo-equilibrium in Table 10. According to Table 10, in Case M_1^1, there exists only one stable pseudo-equilibrium E_1^f. In Case M_2, there exists one stable pseudo-equilibrium E_1^f and one unstable pseudo-equilibrium E_1^e if $\gamma_1>0$, while there exists one stable pseudo-equilibrium E_1^f if $\gamma_1<0$. In Case M_3, there exists one stable pseudo-equilibrium E_1^f and one unstable pseudo-equilibrium E_1^e if $\gamma_1<0$, while there exists one stable pseudo-equilibrium E_1^f if $\gamma_1>0$. In Case M_4^1, there exists one unstable pseudo-equilibrium E_1^e. In Case M_5, there exists one unstable (resp. stable) pseudo-equilibrium E_1^E if $\gamma_1>0$ (resp. $\gamma_1<0$). In Case M_6^1, only one unstable pseudo-equilibrium E_1^F exists for the Filippov system (3).

Up to this point, we have examined the sliding-mode region and the sliding dynamics of Filippov system (3). In fact, Filippov system (3) exhibits quite rich sliding dynamics as the parameters vary, including a series of sliding-mode regions and many pseudo-equilibria. There are a total of seven sliding-mode regions, including $\Sigma_s^1,\Sigma_s^2,\Sigma_s^3,\Sigma_s^4,\Sigma_s^5,\Sigma_s^1\bigcup\Sigma_s^2$ and $\Sigma_s^1\bigcup\Sigma_s^4$, for Filippov system (3). If we choose suitable parameters — for example, the parameters in Cases H_1 and H_4 — two sliding-mode regions Σ_s^1 and Σ_s^2 or Σ_s^1 and Σ_s^4 coexist. For other parameters, only one sliding-mode region, which will take a different form for different parameters, exists for Filippov system (3). The details about the sliding-mode regions and the conditions for each sliding-mode region are listed in Table 2. There exist at most three pseudo-equilibria for Filippov system (3). All possible pseudo-equilibria consist of E_s^a, E_s^b, E_s^c, E_s^A, E_s^B, E_s^D, E_s^e, E_s^f, E_s^E and E_s^F. By choosing suitable parameters, we can derive the existence of a unique pseudo-equilibrium or coexistence of two pseudo-equilibria. Two pseudo-equilibria E_s^b and E_s^c, E_s^A and E_s^c, or E_s^B and E_s^a coexist in Cases Q_1^{11}, Q_1^2 and Q_2^1. We can also get the coexistence of the two pseudo-equilibria E_s^a and E_s^b in Cases P_1^{31} and P_1^4 and the coexistence of E_s^A and E_s^c or E_s^B and E_s^a in case P_2^1. Two pseudo-equilibria E_s^e and E_s^f coexist in case M_2^1 and M_3^2. Three pseudo-equilibria E_s^a, E_s^b and E_s^c coexist for Filippov system (3) in cases Q_1^{42} and P_1^{22}. The detailed results are shown in Theorems 1–3 and Tables 8 and 9, 10.

It is worth emphasizing that the pseudo-equilibrium, as a special equilibrium of Filippov system, plays an important role in the global dynamics of the system. In particular, if the solutions of model (3) eventually approach a pseudo-equilibrium, the number of prostate-cancer cells can be controlled at a predetermined level, which is a desirable outcome.

3.3. Impact of the threshold value on sliding-mode region and pseudo-equilibria

Next we examine the variation of the sliding-mode regions and pseudo-equilibria under different parameter values. To this end, we fix the parameters in Table 1 and parameter β and select two different values for the parameter α in order to explore how the sliding-mode regions and pseudo-equilibria vary, as shown in Fig. 5. Each subplot in Fig. 5 shows the length of sliding-mode region and the number of pseudo-equilibria with different joint threshold value ET. In Fig. 5, the light grey dotted lines represent the crossing region of Σ, while thick dark grey solid lines represent the sliding-mode regions Σ_s. The grey-blue curves and purple curves represent $g_1(X_1,ET)=0$ and $g_2(X_1,ET)=0$, where

$$\begin{aligned}g_1(X_1,ET)=&[r_1(1-u)(\alpha-1)+r_2(\beta-1)]X_1^2-r_2ET^2+[-r_1(1-u)\alpha\\&+r_2(2-\beta)]ETX_1+r_2KET\\&+[r_1(1-u)K-ud_1K-r_2K]X_1,\\g_2(X_1,ET)=&[r_1(\alpha-1)+r_2(\beta-1)]X_1^2-r_2ET^2\\&+[-r_1\alpha+r_2(2-\beta)]ETX_1+r_2KET+(r_1K-r_2K)X_1.\end{aligned}$$

These two curves specify the endpoints of the sliding-mode regions. In fact, the part of any straight line $ET=c$ that falls between these two curves $g_1(X_1,ET)=0$ and $g_2(X_1,ET)=0$ is a sliding-mode region

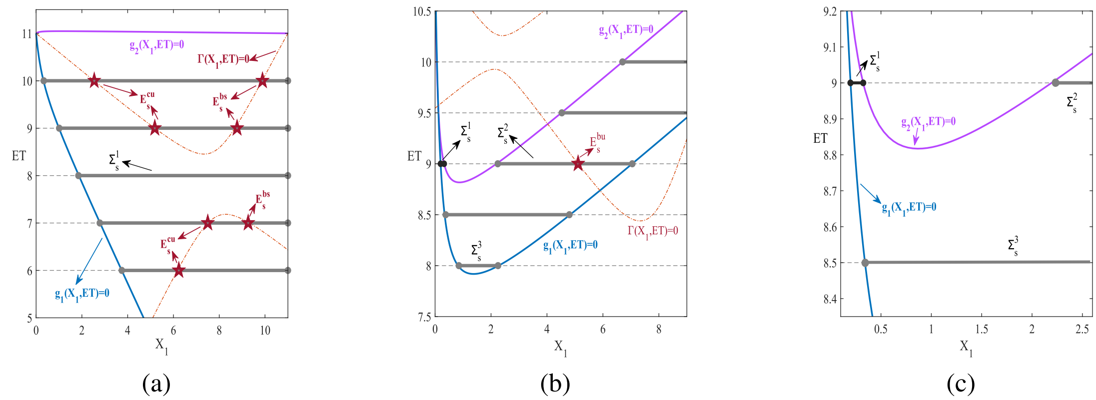

Fig. 5. The sliding-mode regions (thick grey lines) and pseudo-equilibria (red stars) of Filippov system (3) under different parameters α, β and joint threshold value ET. The parameter values are (a) $\alpha = 0.99, \beta = 1.4$, (b) $\alpha = 1.3, \beta = 1.4$ and (c) $\alpha = 1.3, \beta = 1.4$. Subplot (c) is a close-up of subplot (b).

Σ_s, where c represents any positive constant. The red curves represent $\Gamma(X_1) = 0$, in which ET is a variable other than the variable X_1, so we denote these curves as $\Gamma(X_1, ET) = 0$. The intersection points of $\Gamma(X_1, ET) = 0$ and $ET = c$ are pseudo-equilibria provided they lie on the sliding-mode region. The red stars in Fig. 5 indicate the pseudo-equilibria.

When we select the competition coefficient of AC-Ds due to the presence of AC-Is $\alpha = 0.99$ and the competition coefficient of AC-Is due to the presence of AC-Ds $\beta = 1.4$, the sliding-mode regions of Filippov system (3) are shown in Fig. 5(a). There exists one sliding-mode region for different threshold values ET. In this case, Conditions H_6 are satisfied, so the sliding-mode region is Σ_s^1. At the joint threshold value $ET = 7$, two pseudo-equilibria appear on the sliding-mode region Σ_s^1. If the threshold value ET increases (for example, $ET = 8$), the pseudo-equilibrium disappears; i.e., there is no equilibrium on the sliding-mode region. When ET continues to increase (for example, $ET = 9$), there are again two pseudo-equilibria on the sliding-mode region. As the threshold value ET increases further, the sliding-mode region remains as Σ_s^1, although it enlarges.

When we choose the competition coefficients $\alpha = 1.3$ and $\beta = 1.4$, the sliding-mode regions and pseudo-equilibria are as shown in Fig. 5(b). At the joint threshold value $ET = 8$, there is only one sliding-mode region, and no pseudo-equilibrium exists for system (3). In this scenario, Conditions H_2 hold, so the sliding-mode region is Σ_s^3. As ET increases (for example, $ET = 9$), two sliding-mode regions appear for system (3). Then system (3) satisfies Conditions H_1 and the sliding-mode regions take the form Σ_s^1 and Σ_s^2, which we show in thick solid black lines and thick solid grey lines in Fig. 5(b). A pseudo-equilibrium appears on the grey sliding-mode region Σ_s^2. When ET continues to increase (for example, $ET = 9.5$), there is only one sliding-mode region Σ_s^2 for the Filippov system (3) and the pseudo-equilibrium disappears. The existence of two sliding-mode regions Σ_s^1 and Σ_s^2 are shown clearly in Fig. 5(c), which is a close-up of Fig. 5(b).

4. Sliding bifurcation and global dynamics

In this section, we focus our attention on the bifurcation phenomena of Filippov system (3), in which some sliding-mode region is involved. There are four types of equilibria and a special point for Filippov system (3): a real equilibrium, a virtual equilibrium, a pseudo-equilibrium, a boundary equilibrium and a tangent point.

4.1. Equilibria of Filippov system (3)

Regular equilibrium. For system (3), E_1^I is a real equilibrium for $ET > X_{11} + X_{21}$, while it is a virtual equilibrium for $ET < X_{11} + X_{21}$. If $ET < X_1^i + X_2^i$, E_i^{II} is a real equilibrium, while it is a virtual equilibrium for $ET > X_1^i + X_2^i$, where $i \in \{1, 2, 3, 4, 5\}$. Both the real equilibrium and the virtual equilibrium are called regular equilibria, and only those real equilibria can be attractors of the system.

Pseudo-equilibrium. It follows from Section 3 that Filippov system (3) can have at most three pseudo-equilibria $E_S^a(X_1^a, X_2^a)$, $E_S^b(X_1^b, X_2^b)$ and $E_S^c(X_1^c, X_2^c)$ if the conditions in case Q_1^{42} or P_1^{22} hold. Two pseudo-equilibria exist for (3) if the conditions in Cases Q_1^{11}, Q_1^2, Q_2^1, P_1^{31}, P_1^4, P_2^1, M_2^1 or M_3^2 hold. There is only one pseudo-equilibrium if the conditions in other cases listed in Tables 8, Tables 9 and 10 hold.

Boundary equilibrium. The boundary equilibrium of Filippov system (3) satisfies the following condition

$$
\begin{aligned}
&r_1\left(1-\frac{X_1+\alpha X_2}{K}\right)(1-\epsilon u)X_1-(d_1+m_1)\epsilon u X_1=0,\\
&r_2\left(1-\frac{\beta X_1+X_2}{K}\right)X_2+m_1 u\epsilon X_1=0,\\
&X_1+X_2=ET.
\end{aligned}
\tag{17}
$$

Solving (17) yields one boundary equilibrium $E_b^1(X_{11}, X_{21})$ if $ET = X_{11} + X_{21}$. We similarly derive five boundary equilibria $E_B^i(X_1^i, X_2^i)$ if $ET = X_1^i + X_2^i$, where $i = 1, 2, 3, 4, 5$. The boundary equilibria E_b^1 and E_B^i are boundary nodes or boundary foci with $i \in \{1, 4, 5\}$, E_B^2 is a boundary saddle and E_B^3 is a boundary saddle node.

Tangent point. The possible tangent point of Filippov system (3) satisfies the following condition

$$
\begin{aligned}
&r_1(1-\epsilon u)\left(1-\frac{X_1+\alpha X_2}{K}\right)X_1+r_2(1-\frac{\beta X_1+X_2}{K})X_2-d_1\epsilon u X_1=0,\\
&X_1+X_2=ET.
\end{aligned}
\tag{18}
$$

Letting $\epsilon = 0$, we obtain

$$
\begin{aligned}
&r_1\left(1-\frac{X_1+\alpha X_2}{K}\right)X_1+r_2\left(1-\frac{\beta X_1+X_2}{K}\right)X_2=0,\\
&X_1+X_2=ET.
\end{aligned}
\tag{19}
$$

Substituting the second equation of (19) into the first equation, we have

$$
\begin{aligned}
&r_1\left(1-\frac{X_1+\alpha(ET-X_1)}{K}\right)X_1\\
&+r_2\left(1-\frac{\beta X_1+(ET-X_1)}{K}\right)(ET-X_1)=0.
\end{aligned}
$$

It follows that

$$
t_{12}X_1^2+t_{11}X_1+t_{10}=0,
\tag{20}
$$

where

$$
\begin{aligned}
&t_{12}=r_1(\alpha-1)+r_2(\beta-1),\ t_{11}=r_1(K-\alpha ET)+r_2(2ET-\beta ET-K),\\
&t_{10}=r_2(K-ET)ET.
\end{aligned}
$$

Solving (20) gives two roots

$$X_{11}^t = \frac{-t_{11} + \sqrt{t_{11}^2 - 4t_{12}t_{10}}}{2t_{12}}, \quad X_{12}^t = \frac{-t_{11} - \sqrt{t_{11}^2 - 4t_{12}t_{10}}}{2t_{12}}.$$

Thus there are two tangent points $E_t^1(X_{11}^t, X_{21}^t)$ and $E_t^2(X_{12}^t, X_{22}^t)$ for system S_1, where

$$X_{21}^t = ET - X_{11}^t, \quad X_{22}^t = ET - X_{12}^t.$$

When $\epsilon = 1$, we obtain

$$t_{22}X_1^2 + t_{21}X_1 + t_{20} = 0,$$

where

$$t_{22} = r_1(1-u)(\alpha - 1) + r_2(\beta - 1), \qquad t_{20} = r_2(K - ET)ET,$$
$$t_{21} = r_1(1-u)(K - \alpha ET) + r_2(2ET - \beta ET - K) - d_1 u.$$

Solving the above equation with respect to X_1, one can obtain two roots

$$X_{11}^T = \frac{-t_{21} + \sqrt{t_{21}^2 - 4t_{22}t_{20}}}{2t_{22}}, \quad X_{12}^T = \frac{-t_{21} - \sqrt{t_{21}^2 - 4t_{22}t_{20}}}{2t_{22}}.$$

Thus there are two tangent points $E_T^1(X_{11}^T, X_{21}^T)$ and $E_T^2(X_{12}^T, X_{22}^T)$ for system S_2, where

$$X_{21}^T = ET - X_{11}^T, \quad X_{22}^T = ET - X_{12}^T.$$

4.2. Boundary-equilibrium bifurcation of Filippov system (3)

It follows from Section 4.1 that there are six boundary equilibria for system (3). Denote the Jacobians of the free subsystem (5) and the control subsystem (6) as

$$J_1(X_1, X_2) = \begin{bmatrix} r_1\left(1 - \frac{2X_1+\alpha X_2}{K}\right) & -\frac{\alpha}{K}r_1X_1 \\ -\frac{\beta}{K}r_2X_2 & r_2\left(1 - \frac{\beta X_1 + 2X_2}{K}\right) \end{bmatrix}$$

and

$$J_2(X_1, X_2) = \begin{bmatrix} r_1(1-u)\left(1 - \frac{2X_1+\alpha X_2}{K}\right) - (d_1+m_1)u & -\frac{\alpha}{K}r_1(1-u)X_1 \\ -\frac{\beta}{K}r_2X_2 + m_1u & r_2\left(1 - \frac{\beta X_1 + 2X_2}{K}\right) \end{bmatrix},$$

respectively. By the boundary-equilibrium coordinates, we have

$$\det\left(J_1(E_b^1)\right) = r_1r_2\frac{(\alpha-1)(\beta-1)}{1-\alpha\beta} \neq 0,$$

$$\det\left(J_2(E_b^1)\right) = r_1r_2(1-u)\frac{(1-\alpha)(1-\beta)}{1-\alpha\beta} + r_2u(d_1+m_1)\frac{1-\beta}{1-\alpha\beta} + r_1(1-u)\alpha m_1 u\frac{1-\alpha}{1-\alpha\beta}.$$

When $\alpha < 1, \beta < 1$, we have $\det\left(J_2(E_b^1)\right) \neq 0$, so a boundary-node bifurcation occurs at E_b^1 if $ET = X_{11} + X_{12}$; i.e., $ET = \frac{(2-\alpha-\beta)K}{1-\alpha\beta}$. When $\alpha > 1, \beta > 1$, a boundary saddle bifurcation occurs at E_b^1 if $\det\left(J_2(E_b^1)\right) \neq 0$ and $ET = \frac{(2-\alpha-\beta)K}{1-\alpha\beta}$.

Similarly, we have

$$\det\left(J_2(E_B^i)\right) = r_1r_2(1-u)\frac{X_1^iX_2^i}{K^2} + r_1m_1u(1-u)\frac{X_1^i}{K}\left(\frac{X_1^i}{X_2^i} + \alpha\right) > 0,$$

$$\det\left(J_1(E_B^i)\right) = -\frac{2r_1r_2\alpha}{K^2}(X_2^i)^2 + r_1r_2\frac{\alpha - \alpha\beta - 2 + 4Q}{K}X_2^i + r_1r_2(1-\beta Q)(1-2Q),$$

with $i = 1,2,3,4,5$. Let

$$B_2 = -2r_1r_2\alpha, \quad B_1 = r_1r_2(\alpha - \alpha\beta - 2 + 4Q)K, \quad B_0 = r_1r_2(1-\beta Q)(1-2Q)K^2$$

and

$$B_2(X_2)^2 + B_1X_2 + B_0 = 0. \tag{21}$$

Then we have

$$\mathrm{sgn}\left(\det\left(J_1(E_B^i)\right)\right) = \mathrm{sgn}\left(B_2(X_2^i)^2 + B_1X_2^i + B_0\right).$$

Solving (21) with respect to X_2 yields two possible roots:

$$X_{21}^B = \frac{-B_1 + \sqrt{B_1^2 - 4B_2B_0}}{2B_2}, \qquad X_{22}^B = \frac{-B_1 - \sqrt{B_1^2 - 4B_2B_0}}{2B_2}.$$

Then we have the following three possibilities to consider: $B_0 < 0$, $B_0 > 0$ and $B_0 = 0$.

When $B_0 < 0$ holds, one can obtain that $X_{21}^B \cdot X_{22}^B > 0$. If we further have $B_1 > 0$, then $X_{21}^B + X_{22}^B > 0$ holds. It follows that $\det\left(J_1(E_B^i)\right) \neq 0$ if $X_2^i \neq X_{21}^B$ and $X_2^i \neq X_{22}^B$. Therefore, a boundary-equilibrium bifurcation occurs at E_B^i if and only if $ET = X_1^i + X_2^i$ and $X_2^i \neq X_{21}^B$ or $X_2^i \neq X_{22}^B$, where $i = 1,2,3,4,5$. If we further have $B_1 \leq 0$, then $\det\left(J_1(E_1^i)\right) \neq 0$ for all X_2^i since

$$X_{21}^B + X_{22}^B \leq 0 \Longrightarrow X_{2i}^B \leq 0, i = 1,2,$$

in this scenario. Hence, a boundary-equilibrium bifurcation occurs at E_B^i if $ET = X_1^i + X_2^i$ with $i = 1,2,3,4,5$.

When $B_0 > 0$, we have $X_{21}^B < 0$ and $X_{22}^B > 0$, so $\det\left(J_1(E_B^i)\right) \neq 0$ if and only if $X_2^i \neq X_{22}^B$. Then a boundary-equilibrium bifurcation occurs at $E_B^i, i = 1,2,3,4,5$ if $ET = X_1^i + X_2^i$ and $X_2^i \neq X_{22}^B$.

When $B_0 = 0$, one can obtain that $X_{21}^B = 0$ or $X_{22}^B = 0$. If we further have $B_1 > 0$, then $X_{21}^B = 0$ and $X_{22}^B > 0$, so we have $\det\left(J_1(E_1^i)\right) \neq 0$ if and only if $X_2^i \neq X_{22}^B$. Hence, a boundary-equilibrium bifurcation occurs at $E_B^i, i = 1,2,3,4,5,$ if $ET = X_1^i + X_2^i$ and $X_2^i \neq X_{22}^B$. If we further have $B_1 \leq 0$, then $X_{21}^B < 0$ and $X_{22}^B = 0$, so $\det\left(J_1(E_1^i)\right) \neq 0$ holds true for all X_2^i, where $i = 1,2,3,4,5$. Then a boundary-equilibrium bifurcation occurs at $E_B^i, i = 1,2,3,4,5,$ if $ET = X_1^i + X_2^i$.

Hence a series of boundary-equilibrium bifurcations occur for Filippov system (3). A boundary node (focus) bifurcation, boundary saddle bifurcation or boundary saddle-node bifurcation occurs with different parameter values. To better understand the boundary-equilibrium bifurcation, we next demonstrate how it occurs by varying the control parameter ET with all other parameters fixed, as shown Fig. 6. In Fig. 6, the red diamonds represent the saddle points; the red asterisks, red stars and red circles represent nodes, boundary equilibria and trivial equilibria, respectively, which are all the regular real equilibria. The grey thick solid lines and grey thin dashed lines represent the sliding-mode regions and crossing regions, respectively. The orange curves and green curves represent the stable and unstable manifolds of the saddle points E_2^{II}, E_B^2, E_S^b and E_1^I, while the black solid curves are the trajectories of Filippov system (3). When we select threshold value $ET = 8$, we have $ET < X_1^2 + X_2^2 < X_1^1 + X_2^1$, so both E_1^{II} and E_2^{II} are in the region G_2; i.e., they are real. The equilibria E_1^{II} and E_{01} are stable nodes and E_2^{II} is a saddle. The conditions in Case H_2 are satisfied, so the sliding-mode region Σ_3 exists, as shown in Table 2 and Fig. 6(a). As ET increases to the critical value $ET = X_1^2 + X_2^2$ (i.e., $ET = 8.73$), the boundary equilibrium E_B^2 appears, in which $B_0 > 0, B_1 > 0$ and $X_2^2 \neq X_{22}^B$, so a boundary-equilibrium bifurcation occurs, as shown in Fig. 6(b). Then the conditions in Case H_1 are true, so the sliding-mode region takes the form Σ_s^2. As ET continues to increase until it satisfies $X_1^2 + X_2^2 < ET < X_1^1 + X_2^1$, the boundary saddle E_B^2 disappears, in which the conditions in Case Q_1^2 are true, so an unstable pseudo-equilibrium E_S^b appears, as shown in Table 8 and Fig. 6(c), and the sliding-mode region Σ_s^2 still exists. If we increase the threshold value ET to 9.53, the pseudo-equilibrium E_S^b disappears. Direct calculation gives $ET = X_1^1 + X_2^1$, $B_0 > 0, B_1 > 0$ and $X_2^1 \neq X_{22}^B$, so another boundary equilibrium E_B^1 occurs. Then another boundary-equilibrium bifurcation occurs, as shown in Fig. 6(d). When ET continues to increase such that $ET > X_1^1 + X_2^1$, the boundary equilibrium E_B^1 disappears, in which the conditions in Case P_1^1 hold, so the pseudo-equilibrium E_S^c appears, as shown in Table 9 and Fig. 6(e). The real equilibria E_1^I and E_{01} still exist, where E_1^I is a saddle and E_{01} is a stable node.

With the continuous variation of the control threshold ET above, two boundary-equilibrium bifurcations occur for Filippov system (3).

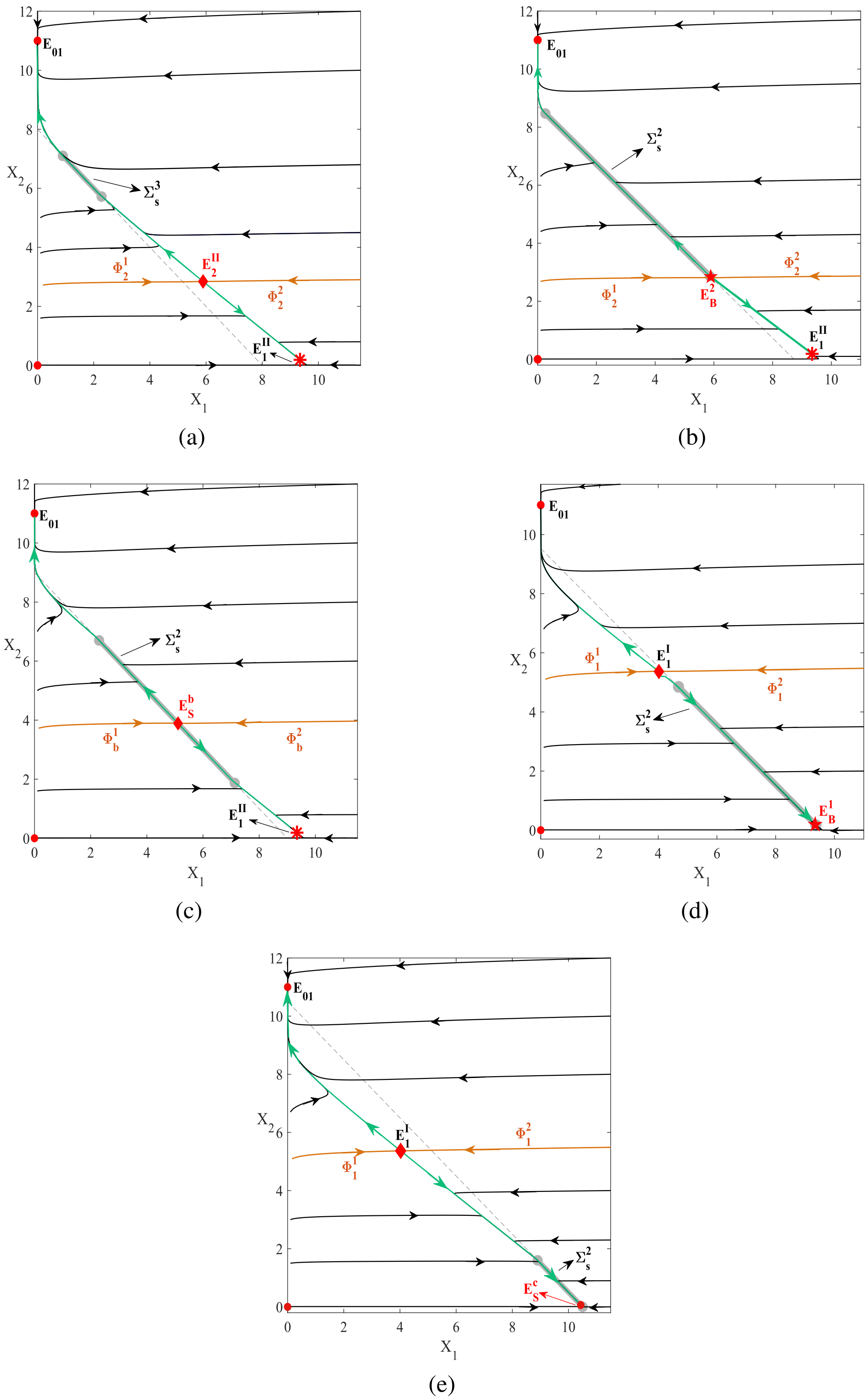

Fig. 6. Boundary-equilibrium bifurcation for Filippov system (3) showing the movement of sliding modes (thick grey lines) and appearance of pseudo-equilibria (red stars). The parameters are $r_1 = 0.5$, $r_2 = 0.006$, $\alpha = 1.3$, $\beta = 1.4$, $u = 0.5$, $d_1 = 0.064$, $m_1 = 0.00005$ and $K = 11$. (a) $ET = 8$, (b) $ET = 8.73$, (c) $ET = 9$, (d) $ET = 9.53$, (e) $ET = 10.5$.

Denoting the values of ET in the five scenarios above as ET_1, ET_2, ET_3, ET_4 and ET_5, we have

$$ET_1 < X_1^2 + X_2^2 = ET_2 < ET_3 < X_1^1 + X_2^1 = ET_4 < ET_5.$$

As ET goes through the variation $ET_1 \longrightarrow ET_2 \longrightarrow ET_3$, the first boundary-equilibrium bifurcation occurs, in which we have the following transformation $E_2^{II} \longrightarrow E_B^2 \longrightarrow E_S^b$; i.e., the real saddle E_2^{II} becomes the boundary saddle E_B^2 first, and second it becomes the unstable pseudo-equilibrium E_S^b, as shown in Fig. 6(a)–(c). Similarly, as ET goes through the variation $ET_3 \longrightarrow ET_4 \longrightarrow ET_5$, the second boundary-equilibrium bifurcation occurs, in which the transformation $E_1^{II} \longrightarrow E_B^1 \longrightarrow E_S^c$ happens; i.e., the real node E_1^{II} becomes the boundary node E_B^1 first, and then it becomes the stable pseudo-equilibrium E_S^c, as shown in Fig. 6(c)–(e). Thus, as ET goes through

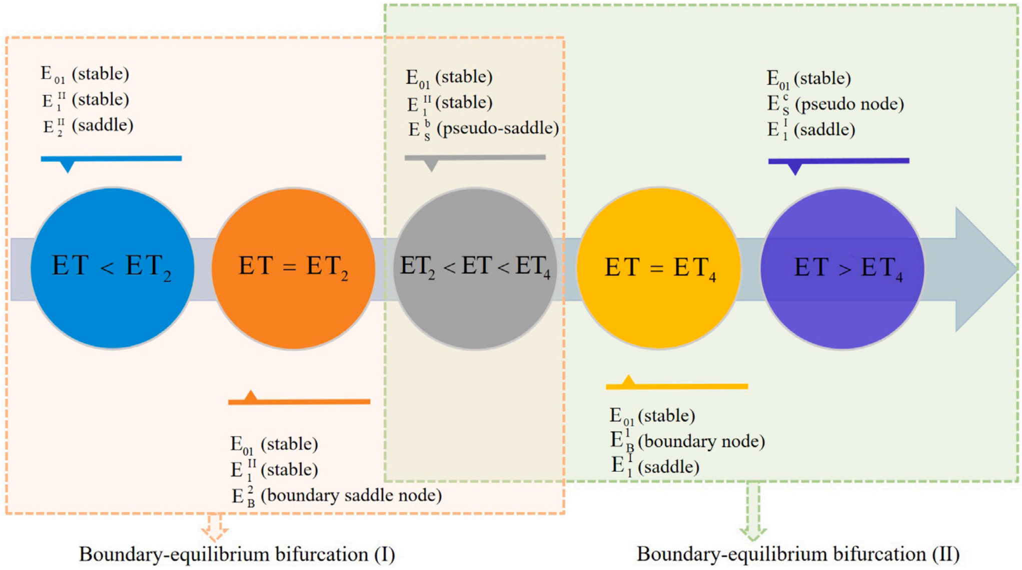

Fig. 7. Flow diagram of the boundary equilibrium bifurcation of Filippov system (3) as the threshold value ET varies.

$ET_1 \longrightarrow ET_2 \longrightarrow ET_3 \longrightarrow ET_4 \longrightarrow ET_5$, two different boundary-equilibrium bifurcations occur. For clarity, we summarize the main result in Fig. 7. In Fig. 7, boundary-equilibrium bifurcation (I)/(II) refers to the first/second boundary-equilibrium bifurcation.

According to the above analysis, small changes in the threshold value ET will cause substantial changes in the dynamic behaviour of Filippov system (3). Fig. 6 shows that when the threshold level is $ET = 8.73$, if the sum of the initial population of AC-Ds and AC-Is is 8.73, then after rapid switching between implementing and suspending ADT, the AC-Is may eventually be contained at a higher level. When the threshold level is greater than 8.73 — for instance, $ET = 9$ — if the sum of the population of AC-Is and AC-Ds is still equal to the threshold value 9, the population of AC-Is may eventually stabilize at a higher level or at a lower level.

4.3. Tangency bifurcation of Filippov system (3)

It follows from Section 3 that there are many sliding-mode regions for Filippov system (3). As the parameters vary, two, one or no sliding-mode regions occur, as shown in Table 2. In the above subsection, we found that a total of four tangent points exist for Filippov system (3). When the number of sliding-mode regions and the tangent points change as the parameters vary, Filippov system (3) will undergo a tangency bifurcation. In the following, we vary the threshold value ET and let other parameters be fixed to illustrate the phenomenon of tangency bifurcation for Filippov system (3), as shown in Fig. 8. In Fig. 8, the grey thick solid lines denote the sliding-mode regions, and the grey circles stand for the tangent points. The competition coefficients between AC-Ds and AC-Is, α and β, are specified as 1.3 and 1.4, respectively, while all other parameters except ET are the same as in Table 1. Then as the threshold value ET varies, a series of tangency bifurcations occur. If the threshold value $ET = 9.4$, Condition H_1 holds, so there exists one sliding-mode region Σ_s^2 with two tangent points E_t^1 and E_T^1 for Filippov system (3), as shown in Table 2 and Fig. 8(a). Case Q_1^2 also holds in this scenario, so an unstable pseudo-equilibrium E_S^b exists with two stable regular equilibria E_{01} and E_1^{II}. If the threshold value ET decreases to 9.25, Condition H_1 also holds, so another sliding-mode region Σ_s^1 appears, although it consists of only one point that is the collision of the two tangent points E_t^2 and E_T^2. This suggests a tangency bifurcation. Thus there are two sliding-mode regions Σ_s^1 and Σ_s^2 for Filippov system (3), as shown in Fig. 8(b). If we continue to decrease the threshold value ET such that $ET = 8.83$, then Condition H_1 holds too, so the sliding-mode region Σ_s^1 expands to a segment with two tangent points E_t^2 and E_T^2 from a collision point, as shown in Fig. 8(c). Thus two sliding-mode regions Σ_s^1, bounded by the two tangent points E_t^2 and E_T^2, and Σ_s^2, bounded by the two tangent points E_t^1 and E_T^1 coexist for Filippov system (3). When ET decreases to 8.82, Condition H_2 holds, so the two tangent points E_t^1 and E_t^2 collide to one regular point, while the two sliding-mode regions Σ_s^1 and Σ_s^2 merge into one sliding-mode region Σ_3 with two tangent points E_T^1 and E_T^2, as shown in Fig. 8(d). This demonstrates a second tangency bifurcation. When ET continues to decrease such that $ET = 8.5$, Condition H_2 is also true, so there is also only one sliding-mode region Σ_s^3, as shown in Fig. 8(e). When the threshold value ET decreases to 7.92, Condition H_2 also holds, so the two tangent points E_T^1 and E_T^2 collide such that the sliding-mode region Σ_s^3 shrinks to one point, as shown in Fig. 8(e). This indicates the occurrence of a third tangency bifurcation. When ET decreases continuously, the sliding-mode region Σ_s^3 disappears.

It is worth emphasizing that when the control threshold ET decreases continuously, as addressed above, three tangency bifurcations occur for Filippov system (3). Let the values of ET in the above six scenarios be $ET_{ci}, i = 1,2,3,4,5,6$, with $ET_{c1} = 9.4$, $ET_{c2} = 9.25$, $ET_{c3} = 8.83$, $ET_{c4} = 8.82$, $ET_{c5} = 8.5$ and $ET_{c6} = 7.92$. Then we have

$$ET_{c1} < ET_{c2} < ET_{c3} < ET_{c4} < ET_{c5} < ET_{c6}.$$

As ET goes through the variation $ET_{c1} \longrightarrow ET_{c2} \longrightarrow ET_{c3}$, the first tangency bifurcation occurs, as shown in Fig. 8(a)–(c). In particular, when $ET = ET_{c2}$, the sliding-mode region Σ_s^1 appears with only one point that is the collision of the two tangent points E_t^2 and E_T^2, so the sliding-mode region becomes $\Sigma_s^1 \bigcup \Sigma_s^2$ from Σ_s^2, as shown in Fig. 8(b). As ET goes through the variation $ET_{c3} \longrightarrow ET_{c4} \longrightarrow ET_{c5}$, the second tangency bifurcation occurs, as shown in Fig. 8(c)–(e). In particular, when $ET = ET_{c4}$, the two tangent points E_t^1 and E_t^2 collide to one point, so the two sliding-mode regions Σ_s^1 and Σ_s^2 merge into one sliding-mode region Σ_s^3, as shown in Fig. 8(d). Similarly, as ET goes through the variation $ET_{c5} \longrightarrow ET_{c6}$, the third tangency bifurcation occurs, as shown in Fig. 8(e)–(f). In particular, when $ET = ET_{c6}$, the two tangent points E_T^1 and E_T^2 collide to one point, so the sliding-mode region Σ_s^3 shrinks to one point, as shown in Fig. 8(f). For clarity, we summarize the main result in the following flow diagram. In Fig. 9, tangency bifurcations (I), (II) and (III) refer to the first, second and third tangency bifurcation, respectively. 'SR' and 'TP' represent the sliding-mode region and the tangent points, respectively.

The above analysis demonstrates that varying the threshold level ET has a significant effect on the evolution of the population of

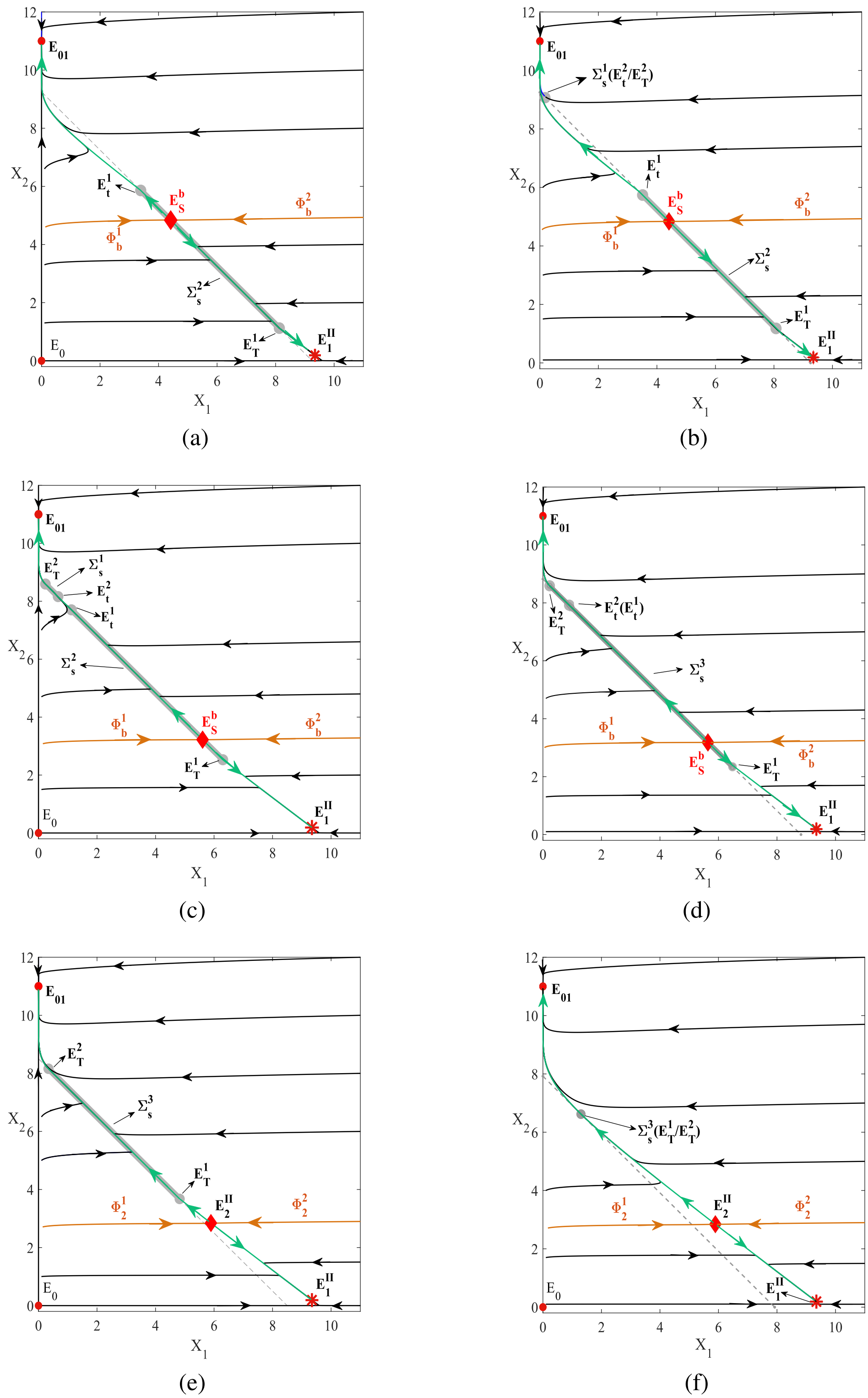

Fig. 8. Tangency bifurcation for Filippov system (3) showing the movement and eventual collapse of the sliding mode (thick grey lines and circles). The parameters are $r_1 = 0.5$, $r_2 = 0.006$, $\alpha = 1.3$, $\beta = 1.4$, $u = 0.5$, $d_1 = 0.064, m_1 = 0.00005$ and $K = 11$. (a) $ET = 9.4$, (b) $ET = 9.25$, (c) $ET = 8.83$, (d) $ET = 8.82$, (e) $ET = 8.5$, (f) $ET = 7.92$.

prostate cancer cells. For example, as shown in Fig. 8, if the threshold level satisfied $ET \geq 9.25$ and the population of AC-Is eventually stabilizes at the level K, then a period of rapid switching between implementing and suspending ADT is initiated before the population of AC-Is goes to the level K. If the threshold level is less than 9.25 — for instance, $ET = 8.83$ — then although the population of AC-Is eventually stabilizes at level K, two periods of rapid switching between implementing and suspending ADT are initiated.

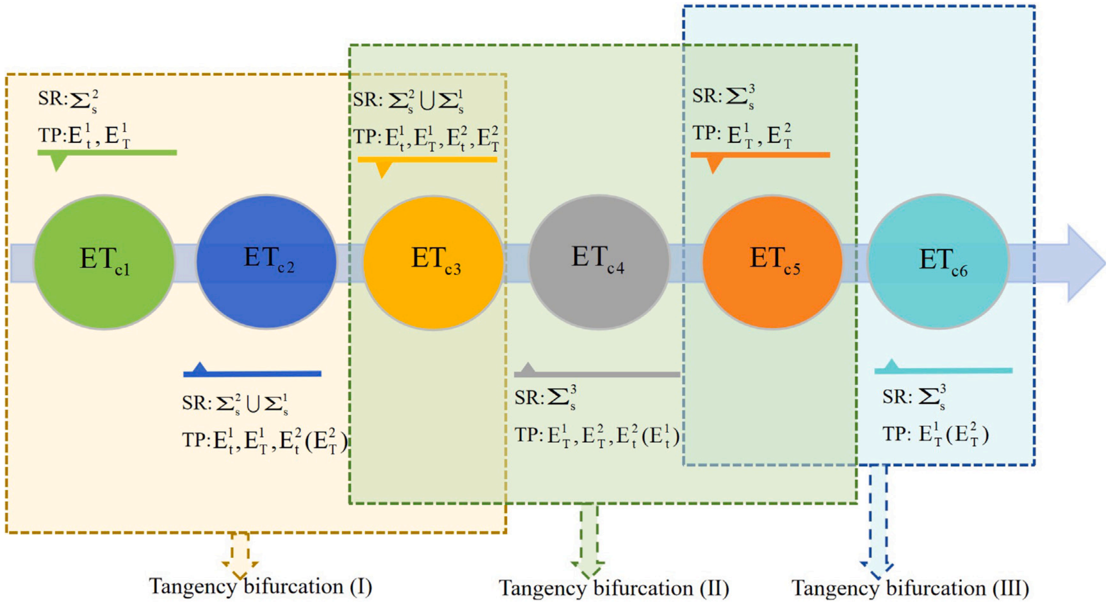

Fig. 9. Flow diagram of the tangency bifurcation of Filippov system (3) with the variation of the threshold value ET.

4.4. Global dynamics of Filippov system (3)

According to Section 2 and Subsection 4.1, there are a total of nine possible regular equilibria for Filippov system (3), including six positive equilibria (E_i^I and $E_i^{II}, i = 1,2,3,4,5$) and three trivial equilibria (E_0, E_{01} and E_{10}). Every real equilibrium can be the attractor of Filippov system (3). There exists a pseudo-equilibrium, and three or two pseudo-equilibria coexist if we choose suitable parameters, while only one pseudo-equilibrium exists in some parameter spaces, as shown in Tables 8, 9 and 10. Among these pseudo-equilibria, some are stable and can be the attractors of Filippov system (3), while the others are unstable. In different parameter spaces, one or two of the seven possible sliding-mode regions $\Sigma_s^1, \Sigma_s^2, \Sigma_s^3, \Sigma_s^4, \Sigma_s^5, \Sigma_s^1 \bigcup \Sigma_s^2$ and $\Sigma_s^1 \bigcup \Sigma_s^4$ exist for Filippov system (3). So as the parameters vary, different sliding-mode regions, regular equilibria and pseudo-equilibria appear, which results in rich dynamics. In the following, we choose the competition coefficients between AC-Ds and AC-Is α, β as 1.3 and 1.4, respectively, while all other parameters except ET are fixed as in Table 1. Then, for different threshold values ET, our targeted model (3) exhibits different behaviour.

When the threshold value $ET = 7.92$, there are four equilibria E_0, E_{01}, E_1^{II} and E_2^{II} for system (3), as shown in Fig. 10(a). The equilibria E_{01} and E_1^{II} are stable nodes, while E_0 and E_2^{II} are saddle points. There is one sliding-mode region, Σ_s^2 with only one point. For convenience, we denote the stable manifolds of the saddle point E_2^{II} as Φ_2^1 and Φ_2^2. Thus Φ_2^1 and Φ_2^2 divide $\mathbb{R}_+^2$ into two subregions. The subregion consisting of all points above (resp. below) Φ_2^1 and Φ_2^2 is denoted as Γ_{21} (resp. Γ_{22}). We denote the initial point of system (3) as $Z_0 \equiv (X_{10}, X_{20})$ in the following. Thus every trajectory starting from $Z_0 \in \Gamma_{21}$ will tend to the regular equilibrium E_{01}, while every trajectory starting from $Z_0 \in \Gamma_{22}$ will tend to the regular equilibrium E_1^{II}, as shown in Fig. 10(a). Hence, we have bistability of the equilibria E_{01} and E_1^{II} in system (3).

When the threshold value increases to $ET = 8$, as shown in Fig. 10(b), the unique sliding-mode region Σ_s^2 becomes longer, which satisfies Condition H_1. The regular equilibria E_{01} and E_1^{II} also are attractors of Filippov system (3). In Fig. 10(c), the threshold value ET increases to 8.83, and two sliding-mode regions Σ_s^1 and Σ_s^2 occur. Both E_{01} and E_1^{II} also exist, which are two stable nodes. There exists one pseudo-equilibrium E_S^b for Filippov system (3), which is a saddle in Case Q_1^2 on the longer sliding-mode region Σ_s^2. Similarly, denote the stable manifolds of pseudo-equilibrium E_S^b as Φ_b^1 and Φ_b^2, which divide $\mathbb{R}_+^2$ into two subregions, Γ_{b1} and Γ_{b2}. Subregion Γ_{b1} (resp. Γ_{b2}) consists of all points above (resp. below) Φ_b^1 and Φ_b^2. Hence every orbit starting from all points $Z_0 \in \Gamma_{b1}$ will tend to the regular equilibrium E_{01}, and every orbit starting from all points $Z_0 \in \Gamma_{b2}$ will tend to another regular equilibrium E_1^{II}. Thus, there are also two attractors, E_1^{II} and E_{01}, for system (3).

When the threshold value ET increases to 9, as shown in Fig. 10(d), the shorter sliding-mode region Σ_s^1 in the above situation disappears, and there is one sliding-mode region Σ_s^2. The unique pseudo-equilibrium E_S^b exists in the form of a saddle, and E_{01} and E_1^{II} are two attractors of Filippov system (3). In Fig. 10(e), the threshold value ET continues to increase to 9.53, and the sliding-mode region Σ_s^2 still exists, but pseudo-equilibrium E_S^b disappears and changes into a regular equilibrium E_1^I, which is a saddle. The regular equilibrium E_1^{II} changes into a boundary equilibrium E_B^1, which is a stable node. Denote the stable manifolds of real equilibrium E_1^I as Φ_1^1 and Φ_1^2; they divide $\mathbb{R}_+^2$ into two subregions, Γ_{11} and Γ_{12}, where Γ_{11} (resp. Γ_{12}) consists of all points above (resp. below) Φ_1^1 and Φ_1^2. Every orbit starting from all points $Z_0 \in \Gamma_{11}$ will tend to the regular equilibrium E_{01}, and every orbit starting from all points $Z_0 \in \Gamma_{12}$ will tend to the boundary equilibrium E_B^1. Hence, we have bistability of the two equilibria, E_B^1 and E_{01}, in system (3).

When the threshold value ET continues to increases to 10.5, as shown in Fig. 10(f). A saddle E_1^I and a stable node E_{01} still exist. Boundary equilibrium E_B^1 disappears, and a stable pseudo-equilibrium E_S^c occurs. Every orbit starting from all points $Z_0 \in \Gamma_{11}$ will tend to the regular equilibrium E_{01}, and every orbit starting from all points $Z_0 \in \Gamma_{12}$ will tend to the pseudo-equilibrium E_S^c. Hence we have bistability of equilibria E_S^c and E_{01} in system (3). For clarity, we summarize the main result in Table 11.

According to the above analysis, the final population of prostate cancer cells not only depends on the threshold level ET but also depends on the population of AC-Ds and AC-Is at the initial moment. Choosing a suitable threshold level ET can contain the population of AC-Is at a very low level in patients whose population of prostate cancer cells in their early treatment can very widely.

5. Discussion

Androgen-deprivation therapy (ADT) is the main method to control prostate cancer, and many models have been established to study the

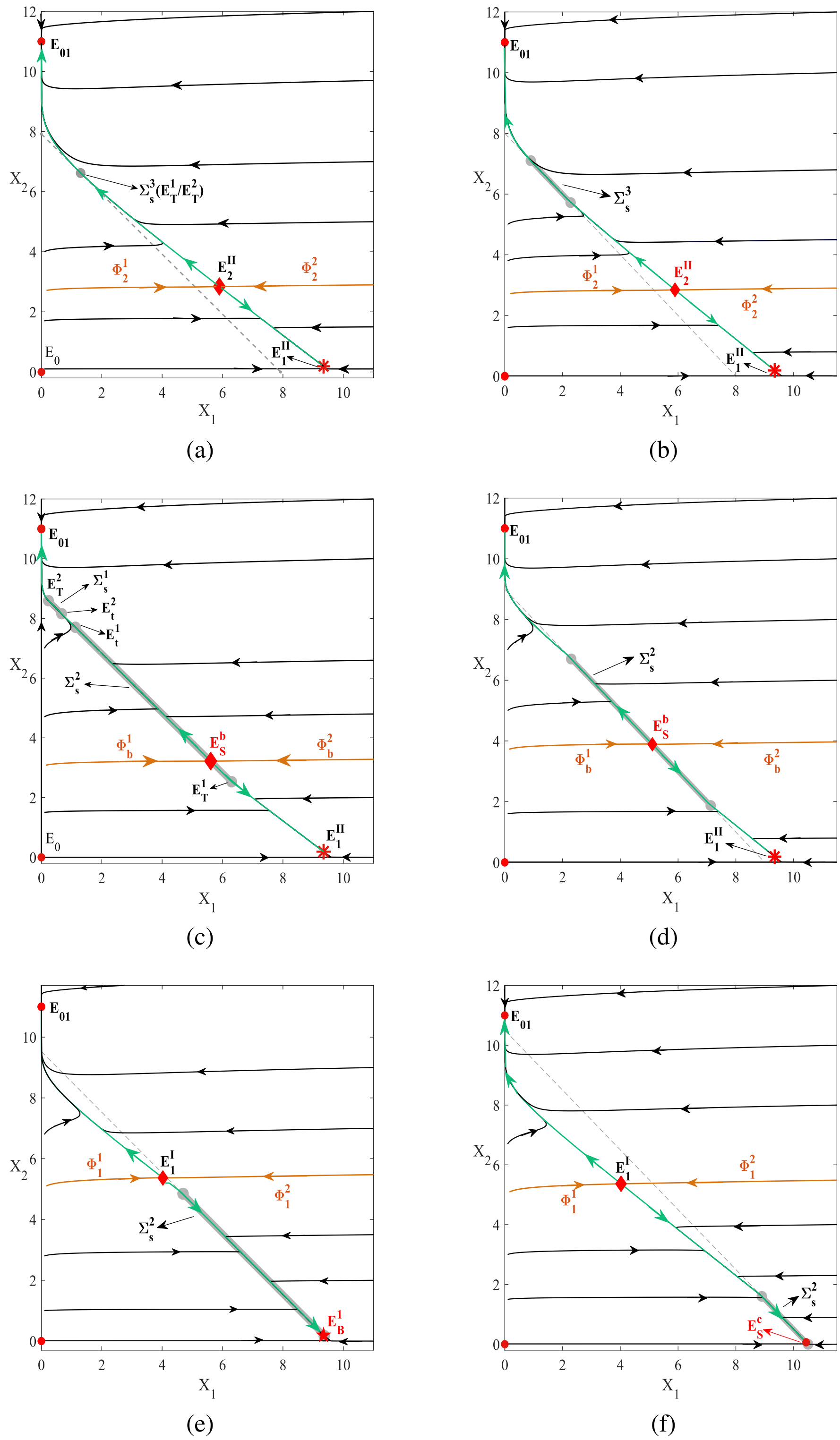

Fig. 10. X_1-X_2 phase plane for Filippov system (3), showing the global dynamics of Filippov system (3). Sliding modes are created, merge and change stability (thick grey lines). The parameters are $r_1 = 0.5$, $r_2 = 0.006$, $\alpha = 1.3$, $\beta = 1.4$, $u = 0.5$, $d_1 = 0.064$, $m_1 = 0.00005$ and $K = 11$. (a) $ET = 7.92$, (b) $ET = 8$, (c) $ET = 8.83$, (d) $ET = 9$, (e) $ET = 9.53$, (f) $ET = 10.5$.

effect of ADT in controlling the development of the prostate cancer. These models mainly focus on the efficacy of continuous therapy, but intermittent androgen-deprivation therapy (IADT) plays a vital role in the treatment. In this study, we establish a type of novel non-smooth model to mimic the effect of IADT to combat the development of ADT by introducing a joint piecewise-defined control function. The joint control measure is defined as follows: ADT is carried out once the total population of androgen-dependent cells and androgen-independent cells (AC-Is) of the patients exceeds the threshold value ET, while the treatment is suspended once the population of cancer cells is below ET.

We first analysed the existence of all possible equilibria for the free-subsystem and control-subsystem and then examined the dynamics of the two subsystems. The sliding-mode region as well as the sliding

Table 11
Attractors, attraction regions and sliding-mode regions for Filippov system (3) with the variation of threshold values.

Threshold values	Sliding-mode regions	Attractors with attraction regions
$ET = 7.92$	$\Sigma_s^3(E_T^1/E_T^2)$	$E_{01}(\Gamma_{21})$, $E_1^{II}(\Gamma_{22})$, $E_2^{II}(\Phi_2^1 \bigcup \Phi_2^2)$
$ET = 8$	Σ_s^3	$E_{01}(\Gamma_{21})$, $E_1^{II}(\Gamma_{22})$, $E_2^{II}(\Phi_2^1 \bigcup \Phi_2^2)$
$ET = 8.83$	$\Sigma_s^2 \bigcup \Sigma_s^1$	$E_{01}(\Gamma_{b1})$, $E_1^{II}(\Gamma_{b2})$, $E_s^b(\Phi_b^1 \bigcup \Phi_b^2)$
$ET = 9$	Σ_s^2	$E_{01}(\Gamma_{b1})$, $E_1^{II}(\Gamma_{b2})$, $E_s^b(\Phi_b^1 \bigcup \Phi_b^2)$
$ET = 9.53$	Σ_s^2	$E_{01}(\Gamma_{11})$, $E_B^1(\Gamma_{12})$, $E_1^1(\Phi_1^1 \bigcup \Phi_1^2)$
$ET = 10.5$	Σ_s^2	$E_{01}(\Gamma_{11})$, $E_S^c(\Gamma_{12})$, $E_1^1(\Phi_1^1 \bigcup \Phi_1^2)$

dynamics are discussed for the proposed Filippov system. We found that seven possible sliding-mode regions may occur for our targeted system. As the parameters vary, there are either one or two sliding-mode regions for the targeted system. Two pieces of sliding-mode regions coexist for system (3) if certain conditions are satisfied; while two other pieces of sliding-mode regions exist if other conditions are satisfied. In different parameter space, there are one, two or at most three pseudo-equilibria for the targeted Filippov system. The most interesting is that a total of three pseudo-equilibria can coexist under certain conditions; one of these pseudo-equilibria is stable, while the other two pseudo-equilibria are unstable. These three pseudo-equilibria also exist for our targeted Filippov system when other conditions hold, where two of them are stable and the other is unstable. The conditions and stability of all pseudo-equilibria are shown in Tables 8, 9 and 10. Biologically, the existence of a sliding-mode region provides the possibility of a rapid alternation of initiating ADT while suspending ADT and vice versa, which leads to shorter periods of both modalities. The existence of a stable pseudo-equilibrium suggests that the population of prostate cancer cells can be curbed at a predetermined level.

A series of boundary-equilibrium bifurcations — including a boundary-node (focus) bifurcation, a boundary-saddle bifurcation and a boundary–saddle-node bifurcation — occur for our targeted Filippov system. In particular, as the threshold value ET increases from ET_1 to ET_5, two boundary-equilibrium bifurcations (i.e., a boundary saddle bifurcation and a boundary-node bifurcation) occur for the targeted Filippov system. As the threshold value ET varies, the number of sliding-mode regions and tangent points will change, resulting in a series of tangency bifurcations for targeted Filippov system. As ET decreases from ET_{c1} to ET_{c6}, the targeted Filippov system undergoes a total of three tangency bifurcations, in which one sliding-mode region changes to two sliding-mode regions, or these two sliding-mode regions merge into one sliding-mode region, or the sliding-mode region shrinks to a single point. These phenomena indicate that small changes in the threshold value will cause substantial changes in the dynamic behaviour of the targeted Filippov system. In particular, small changes in ET result in a variation of the attractors or the sliding mode regions, which suggests a variation of procession dynamics or a stabilized level of the population of prostate cancer cells occurring as the threshold value crosses the critical value.

Due to the complexity of the dynamics for Filippov system (3), it is hard to theoretically determine the global dynamics in the whole parameter space, and our numerical simulations show some special cases, in which we have addressed the coexistence of three equilibria as well as the bistability of two equilibria. With different threshold values and initial states, the trajectory of the targeted Filippov system ultimately approaches the trivial equilibrium, one of the regular equilibria, one of the boundary equilibria or the pseudo-equilibrium. The main findings indicate that the population of AC-Is can be contained at a relatively low level or a predetermined level if its initial value is below the critical value and a proper threshold value is chosen. We can further choose a threshold such that the rapid alternation of activating ADT and suspending ADT is required for one period, two periods or no period of time before the population of prostate cancer cells stabilizes. This is related to studies focused on optimal schedules of treatment or on whether cancer cells can be eliminated. For example, Pei et al. [20] proposed optimal durations of on- and off-treatment and chemotherapy dosages. Hirata et al. [23] found that for those patients, the relapse of prostate cancer can be delayed by IADT compared with CADT, but that IADT cannot stabilize the origin where no cancer cells exist. In contrast to these studies, we have proposed strategies to contain the prostate cancer cells at a specified level when elimination is not possible.

Our model has several limitations, which should be acknowledged. We ignore the possibility of back mutation in our model, which we will consider in future work. Filippov systems are an approximate description of the switching between two distinctive control measures in the real world after a threshold is reached; a piecewise model with a threshold window constituted by a lower threshold and an upper threshold could better mimic real-world activation. This would result in a system that is different and much less smooth than the Filippov system. Treatment may also work asymmetrically for AC-Ds versus AC-Is, which can be mimicked by a more detailed model and will be addressed in a future study.

We focused on the effect of the IADT in controlling prostate cancer, which leads to a Filippov model with a joint threshold. The main results obtained in this work indicate that we can choose an appropriate joint threshold such that as few AC-Ds mutate into AC-Is as possible and that we can reduce the population of AC-Ds and AC-Is as much as possible after IADT treatment. Designing such treatment schedules could greatly ease the burden of prostate-cancer treatment and vastly increase patient quality of life.

CRediT authorship contribution statement

Aili Wang: Writing – review & editing, Validation, Supervision, Project administration, Methodology, Investigation, Funding acquisition, Conceptualization. **Rong Yan:** Writing – original draft, Software, Resources, Formal analysis, Data curation. **Haixia Li:** Resources, Methodology, Data curation. **Xiaodan Sun:** Visualization, Resources, Data curation. **Weike Zhou:** Resources, Data curation. **Stacey R. Smith?:** Writing – review & editing, Visualization, Supervision, Project administration.

Declaration of competing interest

The authors declare no conflict of interest.

Acknowledgements

The authors are grateful to Cassandra Wooldridge for discussions. AW was supported by the National Natural Science Foundation of China (NSFC, 12271431, 12371404), XS was supported by the National Natural Science Foundation of China (NSFC, 12071366), WZ was supported by the National Natural Science Foundation of China (NSFC, 12001349), SS? was supported by an NSERC Discovery Grant. For citation purposes, please note that the question mark in "Smith?" is part of her name.

Appendix A. Existence of pseudo-equilibrium for the case $\gamma_0 > 0$

In the following, we examine the existence of all possible pseudo-equilibria and their stability for $\gamma_0 < 0$ by implementing a similar analysis for the case $\gamma_0 > 0$. In this case, there are also three scenarios.

Case P_1: $\gamma_0 < 0, N < 0$. In this case, there also exist three roots X_1^a, X_1^b and X_1^c for $\Gamma(X_1) = 0$, and we have the following four further possibilities to consider according to the sign of γ_3 and γ_2.

Case P_1^1: $\gamma_3 > 0, \gamma_2 \geq 0$. In this case, two negative roots and one positive root (i.e., X_1^c) exist for $\Gamma(X_1) = 0$ since $X_1^a + X_1^b + X_1^c \leq 0$ and $X_1^a \cdot X_1^b \cdot X_1^c > 0$. Performing a similar analysis to Case Q_1, we get the detailed conditions for the existence of one positive root and describe them in Table 12.

Case P_1^2: $\gamma_3 > 0, \gamma_2 < 0$. In this case, there exist two negative roots and one positive root (i.e., X_1^c) or three positive roots (i.e., X_1^a, X_1^b and X_1^c) since $X_1^a + X_1^b + X_1^c > 0$ and $X_1^a \cdot X_1^b \cdot X_1^c > 0$. One positive root or three positive roots exist if one of the following conditions are satisfied:

Table 12
Conditions for the existence of one positive root in Case P_1^1.

$N < 0, \gamma_0 < 0$	$\alpha < 1, \beta < 1$	$\gamma_{21} > 0, \gamma_{20} > 0$, for all ET $\gamma_{21} > 0, \gamma_{20} < 0, ET > -\frac{\gamma_{20}}{\gamma_{21}}$ $\gamma_{21} < 0, \theta_{20} > 0, 0 < ET < -\frac{\gamma_{20}}{\gamma_{21}}$ $ET = -\frac{\gamma_{20}}{\gamma_{21}}$
	$\alpha > 1, \beta > 1$	$\gamma_{21} > 0, \gamma_{20} > 0$, for all ET $\gamma_{21} > 0, \gamma_{20} < 0, ET > -\frac{\gamma_{20}}{\gamma_{21}}$ $\gamma_{21} < 0, \theta_{20} > 0, 0 < ET < -\frac{\gamma_{20}}{\gamma_{21}}$ $ET = -\frac{\gamma_{20}}{\gamma_{21}}$

Table 13
Conditions for the existence of positive roots in Case P_1^2.

Conditions			Number of roots
$\gamma_0 < 0, N < 0$	$\alpha < 1, \beta < 1, \gamma_1 < 0$	$\gamma_{21} > 0, \gamma_{20} < 0, 0 < ET < -\frac{\gamma_{20}}{\gamma_{21}}$ $\gamma_{21} < 0, \gamma_{20} > 0, ET > -\frac{\gamma_{20}}{\gamma_{21}}$ $\gamma_{21} < 0, \gamma_{20} < 0$, for all ET	One
	$\alpha > 1, \beta > 1, \gamma_1 < 0$	$\gamma_{21} > 0, \gamma_{20} < 0, 0 < ET < -\frac{\gamma_{20}}{\gamma_{21}}$ $\gamma_{21} < 0, \gamma_{20} > 0, ET > -\frac{\gamma_{20}}{\gamma_{21}}$ $\gamma_{21} < 0, \gamma_{20} < 0$, for all ET	
	$\alpha < 1, \beta < 1, \gamma_1 > 0$	$\gamma_{21} > 0, \gamma_{20} < 0, 0 < ET < -\frac{\gamma_{20}}{\gamma_{21}}$ $\gamma_{21} < 0, \gamma_{20} > 0, ET > -\frac{\gamma_{20}}{\gamma_{21}}$ $\gamma_{21} < 0, \gamma_{20} < 0$, for all ET	Three
	$\alpha > 1, \beta > 1, \gamma_1 > 0$	$\gamma_{21} > 0, \gamma_{20} < 0, 0 < ET < -\frac{\gamma_{20}}{\gamma_{21}}$ $\gamma_{21} < 0, \gamma_{20} > 0, ET > -\frac{\gamma_{20}}{\gamma_{21}}$ $\gamma_{21} < 0, \gamma_{20} < 0$, for all ET	

- $\alpha < 1, \beta < 1, \gamma_{21} > 0, \gamma_{20} < 0, 0 < ET < -\frac{\gamma_{20}}{\gamma_{21}}$;
- $\alpha < 1, \beta < 1, \gamma_{21} < 0, \gamma_{20} < 0$;
- $\alpha < 1, \beta < 1, \gamma_{21} < 0, \gamma_{20} > 0, ET > -\frac{\gamma_{20}}{\gamma_{21}}$;
- $\alpha > 1, \beta > 1, \gamma_{21} > 0, \gamma_{20} < 0, 0 < ET < -\frac{\gamma_{20}}{\gamma_{21}}$;
- $\alpha > 1, \beta > 1, \gamma_{21} < 0, \gamma_{20} < 0$;
- $\alpha > 1, \beta > 1, \gamma_{21} < 0, \gamma_{20} > 0, ET > -\frac{\gamma_{20}}{\gamma_{21}}$.

By solving $\Gamma'(X_1) = 0$ with respect to X_1, we get two roots, the smaller of which is

$$X'_{12} = \frac{-\gamma_2 - \sqrt{\gamma_2^2 - 3\gamma_3\gamma_1}}{3\gamma_3}.$$

If $X'_{12} < 0$, there is one positive root for (13), while there are three positive roots if $X'_{12} > 0$. Direct calculation yields that $X'_{12} < 0$ for $\gamma_1 < 0$ and $X'_{12} > 0$ for $\gamma_1 > 0$. Concluding the above discussion, we derive the conditions for the existence of one positive root, which we denote as P_1^{21}, and the conditions for three positive roots, which we denote as P_1^{22}, and summarize them in Table 13.

Case P_1^3: $\gamma_3 < 0, \gamma_2 < 0$. In this case, there exist one negative root and two positive roots (i.e., X_1^a and X_1^b) or three negative roots. Whether there are two positive roots in this scenario depends on the sign of the larger root of $\Gamma'(X_1) = 0$; i.e.,

$$X'_{12} = \frac{-\gamma_2 - \sqrt{\gamma_2^2 - 3\gamma_3\gamma_1}}{3\gamma_3}.$$

If $X'_{12} > 0$, there are two positive roots. $X'_{12} > 0$ if $\gamma_1 > 0$, so we denote the conditions ($\gamma_0 < 0, N < 0, \gamma_3 < 0, \gamma_2 < 0, \gamma_1 > 0$) for two positive roots as P_1^{31}. Similarly, we obtain the conditions for the existence of two positive roots and summarize these results in Table 14.

Case P_1^4: $\gamma_3 < 0, \gamma_2 \geq 0$. Similarly, there exist two positive roots (i.e., X_1^a and X_1^b) and one negative root for (13). We derive the conditions to guarantee the existence of two positive roots and summarize them in Table 15.

Case P_2: When $N = 0$, there are three real roots for (13). There are a total of two distinct real roots, including a root of multiplicity two and a single root if we further have $n_1 \neq 0, n_0 \neq 0$; otherwise, there is only one real root which is of multiplicity three. Similar to Case P_1, we get the conditions for the existence of two distinct real roots X_1^A, X_1^c or X_1^B, X_1^a, which are $N = 0, \gamma_0 < 0, n_1 \neq 0, n_0 \neq 0, \gamma_1 > 0, \gamma_3 > 0, \gamma_2 < 0$. We summarize them in Table 16. For convenience, we denote them as Condition P_2^1 below. We similarly get the conditions for the existence of only one positive real root of multiplicity three X_1^D by replacing the conditions $n_1 \neq 0, n_0 \neq 0$ with $n_1 = 0, n_0 = 0$. We denote this set of conditions as P_2^2 below. Similarly, there is only one positive root X_1^c if

$$N = 0, \gamma_0 < 0, n_1 \neq 0, n_0 \neq 0, \gamma_3 > 0, \gamma_2 \geq 0$$

or

$$N = 0, \gamma_0 < 0, n_1 \neq 0, n_0 \neq 0, \gamma_1 < 0, \gamma_3 > 0, \gamma_2 < 0$$

holds true, which we denote as Q_2^3 and Q_2^4 below. There exists one positive root X_1^A of multiplicity two, if

$$N = 0, \gamma_0 < 0, n_1 \neq 0, n_0 \neq 0, \gamma_3 < 0, \gamma_2 < 0$$

or

$$N = 0, \gamma_0 < 0, n_1 \neq 0, n_0 \neq 0, \gamma_1 < 0, \gamma_3 < 0, \gamma_2 \geq 0$$

holds true, which we denote as Q_2^5 and Q_2^6.

Case P_3: When $N > 0$, there is one real root and two imaginary roots for $\Gamma(X_1) = 0$. According to (14), the unique real root of (15) is positive when $\gamma_3 > 0$. Direct calculation gives $\gamma_3 > 0$ if $\alpha > 1, \beta > 1$ or $\alpha < 1, \beta < 1$.

Table 14
Conditions for the existence of two positive roots in Case P_1^3.

$\gamma_0 < 0, N < 0$	$\alpha > 1, \beta < 1, \gamma_1 > 0$	$\gamma_{21} > 0, \gamma_{20} < 0, 0 < ET < -\frac{\gamma_{20}}{\gamma_{21}}$ $\gamma_{21} < 0, \gamma_{20} > 0, ET > -\frac{\gamma_{20}}{\gamma_{21}}$ $\gamma_{21} < 0, \gamma_{20} < 0$, for all ET
	$\alpha < 1, \beta > 1, \gamma_1 > 0$	$\gamma_{21} > 0, \gamma_{20} < 0, 0 < ET < -\frac{\gamma_{20}}{\gamma_{21}}$ $\gamma_{21} < 0, \gamma_{20} > 0, ET > -\frac{\gamma_{20}}{\gamma_{21}}$ $\gamma_{21} < 0, \gamma_{20} < 0$, for all ET

Table 15
Conditions of the existence of two positive roots in Case P_1^4.

$\gamma_0 < 0, N < 0$	$\alpha > 1, \beta < 1$	$\gamma_{21} > 0, \gamma_{20} > 0$, for all ET $\gamma_{21} > 0, \gamma_{20} < 0, ET > -\frac{\gamma_{20}}{\gamma_{21}}$ $\gamma_{21} < 0, \gamma_{20} > 0, 0 < ET < -\frac{\gamma_{20}}{\gamma_{21}}$ $ET = -\frac{\gamma_{20}}{\gamma_{21}}$
	$\alpha < 1, \beta > 1$	$\gamma_{21} > 0, \gamma_{20} > 0$, for all ET $\gamma_{21} > 0, \gamma_{20} < 0, ET > -\frac{\gamma_{20}}{\gamma_{21}}$ $\gamma_{21} < 0, \gamma_{20} > 0, 0 < ET < -\frac{\gamma_{20}}{\gamma_{21}}$ $ET = -\frac{\gamma_{20}}{\gamma_{21}}$

Table 16
Conditions for the existence of two distinct positive real roots for Case P_2.

$\gamma_0 < 0, N = 0, n_1 \neq 0, n_0 \neq 0$	$\alpha < 1, \beta < 1, \gamma_1 > 0$	$\gamma_{21} > 0, \gamma_{20} < 0, 0 < ET < -\frac{\gamma_{20}}{\gamma_{21}}$ $\gamma_{21} < 0, \gamma_{20} < 0$, for all ET $\gamma_{21} < 0, \gamma_{20} > 0, ET > -\frac{\gamma_{20}}{\gamma_{21}}$
	$\alpha > 1, \beta > 1, \gamma_1 > 0$	$\gamma_{21} > 0, \gamma_{20} < 0, 0 < ET < -\frac{\gamma_{20}}{\gamma_{21}}$ $\gamma_{21} < 0, \gamma_{20} < 0$, for all ET $\gamma_{21} < 0, \gamma_{20} > 0, ET > -\frac{\gamma_{20}}{\gamma_{21}}$

Appendix B. Existence of pseudo-equilibrium for the case $\gamma_0 = 0$

We next examine the existence of pseudo-equilibria for the Filippov system (3) when $\gamma_0 = 0$. To this end, it is necessary to solve the positive root of Eq. (13). We only need to analyse the positive roots of the following equation

$$\gamma_3 X_1^2 + \gamma_2 X_1^1 + \gamma_1 = 0. \tag{22}$$

Denote $\Omega = \gamma_2^2 - 4\gamma_3\gamma_1$. When $\Omega > 0$, there are two roots X_1^e and X_1^f for (22), while there is only one root X_1^E if $\gamma_2 = 0$, where

$$X_1^e = \frac{-\gamma_2 - \sqrt{\gamma_2^2 - 4\gamma_3\gamma_1}}{2\gamma_3}, \quad X_1^f = \frac{-\gamma_2 + \sqrt{\gamma_2^2 - 4\gamma_3\gamma_1}}{2\gamma_3}, \quad X_1^E = \sqrt{\frac{-\gamma_1}{\gamma_3}},$$

which satisfy $X_1^e + X_1^f = -\frac{\gamma_2}{\gamma_3}, X_1^e \cdot X_1^f = \frac{\gamma_1}{\gamma_3}$. So we have five further cases to consider according to the sign of γ_1, γ_2 and γ_3.

Case M_1: $\gamma_3 > 0, \gamma_2 > 0$. In this scenario, we have $X_1^e + X_1^f \leq 0$ since $-\frac{\gamma_2}{\gamma_3} \leq 0$. When $\gamma_1 > 0$, we have $X_1^e \cdot X_1^f > 0$ since $\frac{\gamma_1}{\gamma_3} > 0$, so both X_1^e and X_1^f are negative. When $\gamma_1 < 0$, we have $X_1^e \cdot X_1^f < 0$, so there is one positive root X_1^f and one negative root X_1^e for (22). We denote these conditions ($\gamma_0 = 0, \Omega > 0, \gamma_3 > 0, \gamma_2 > 0, \gamma_1 < 0$) for the existence of one positive root (i.e., X_1^f) as Case M_1^1. Further investigation yields that X_1^f is a positive root for (22) if $\alpha < 1, \beta < 1$ and one of the following conditions holds:

(M_1^a) $\gamma_{21} > 0, \gamma_{20} > 0$;
(M_1^b) $\gamma_{21} > 0, \gamma_{20} < 0, ET > -\frac{\gamma_{20}}{\gamma_{21}}$;
(M_1^c) $\gamma_{21} < 0, \gamma_{20} > 0, 0 < ET < -\frac{\gamma_{20}}{\gamma_{21}}$.

We similarly derive that X_1^f is the unique positive root if $\alpha > 1, \beta > 1$ and one of (M_1^s), $s \in \{a, b, c\}$ is true.

Case M_2: $\gamma_3 > 0, \gamma_2 < 0$. In this scenario, $X_1^e + X_1^f > 0$ since $-\frac{\gamma_2}{\gamma_3} > 0$. When $\gamma_1 > 0$, we have $X_1^e \cdot X_1^f > 0$ since $\frac{\gamma_1}{\gamma_3} > 0$, so both X_1^e and X_1^f are positive roots of (22). When $\gamma_1 < 0$, it follows that $X_1^e \cdot X_1^f < 0$ since $\frac{\gamma_1}{\gamma_3} < 0$, so there is only one positive root X_1^f of (22). We denote the conditions to guarantee two positive roots (resp. one positive root) — i.e., $\gamma_0 = 0, \Omega > 0, \gamma_3 > 0, \gamma_2 < 0, \gamma_1 > 0$ (resp. $\gamma_0 = 0, \Omega > 0, \gamma_3 > 0, \gamma_2 < 0, \gamma_1 < 0$) — as Case M_2^1 (resp.M_2^2). There are two (resp. one) positive roots — i.e., X_1^e and X_1^f (resp. X_1^f) — if $\alpha < 1, \beta < 1, \gamma_1 > 0$ (resp. $\gamma_1 < 0$) and one of the following conditions hold:

(M_2^a) $\gamma_{21} > 0, \gamma_{20} < 0, 0 < ET < -\frac{\gamma_{20}}{\gamma_{21}}$;
(M_2^b) $\gamma_{21} < 0, \gamma_{20} < 0$, for all ET;
(M_2^c) $\gamma_{21} < 0, \gamma_{20} > 0, ET > -\frac{\gamma_{20}}{\gamma_{21}}$.

Similarly, X_1^e and X_1^f are positive roots for (22) if $\alpha > 1, \beta > 1$ and $\gamma_1 > 0$, while only X_1^f is a positive root for (22) if $\alpha > 1, \beta > 1$ and $\gamma_1 < 0$.

Case M_3: $\gamma_3 < 0, \gamma_2 > 0$. In this scenario, we have $X_1^e + X_1^f > 0$ since $-\frac{\gamma_2}{\gamma_3} > 0$. If we further have $\gamma_1 > 0$, then $X_1^e \cdot X_1^f < 0$ since $\frac{\gamma_1}{\gamma_3} < 0$, so there is only one positive root X_1^f of Eq. (22). If we have $\gamma_1 < 0$, then $X_1^e \cdot X_1^f > 0$ since $\frac{\gamma_1}{\gamma_3} > 0$, so both X_1^e and X_1^f are positive roots of Eq. (22). We similarly denote the conditions for one positive root (resp. two positive roots) — i.e., $\gamma_0 = 0, \Omega > 0, \gamma_3 < 0, \gamma_2 > 0, \gamma_1 > 0$ (resp., $\gamma_0 = 0, \Omega > 0, \gamma_3 < 0, \gamma_2 > 0, \gamma_1 < 0$) — as Case M_3^1 (resp. M_3^2) below. There are two positive roots (X_1^e, X_1^f) of (22) if $\alpha > 1, \beta < 1, \gamma_1 < 0$ and one of the following conditions hold:

(M_3^a) $\gamma_{21} > 0, \gamma_{20} < 0$, for all ET;
(M_3^b) $\gamma_{21} > 0, \gamma_{20} < 0, ET > -\frac{\gamma_{20}}{\gamma_{21}}$;
(M_3^c) $\gamma_{21} < 0, \gamma_{20} > 0, 0 < ET < -\frac{\gamma_{20}}{\gamma_{21}}$.

We similarly find that there are also two positive roots X_1^e and X_1^f of (22) if $\alpha < 1, \beta > 1, \gamma_1 < 0$ and one of (M_3^s), $s \in \{a, b, c\}$ are true; there is one positive root X_1^f of (22) if $\gamma_1 > 0, \alpha > 1, \beta < 1$ and one of (M_3^s), $s \in \{a, b, c\}$ are true; X_1^f is also the unique positive root for (22) if $\gamma_1 > 0, \alpha < 1, \beta > 1$ and one of (M_3^s), $s \in \{a, b, c\}$ are true.

Case M_4: $\gamma_3 < 0, \gamma_2 < 0$. In this scenario, $X_1^e + X_1^f < 0$ since $-\frac{\gamma_2}{\gamma_3} < 0$. If we further have $\gamma_1 > 0$, then $X_1^e \cdot X_1^f < 0$ since $\frac{\gamma_1}{\gamma_3} < 0$, so there exists one positive root X_1^e of (22). If $\gamma_1 < 0$, we have $X_1^e \cdot X_1^f > 0$ since $\frac{\gamma_1}{\gamma_3} > 0$, so both X_1^f and X_1^f are negative. We denote the conditions $\gamma_0 = 0, \Omega > 0, \gamma_3 < 0, \gamma_2 < 0, \gamma_1 > 0$ as Case M_4^1. There is one positive root X_1^e of (22) if $\alpha < 1, \beta > 1, \gamma_1 > 0$ and one of the following conditions hold:

(M_4^a) $\gamma_{21} > 0, \gamma_{20} < 0, 0 < ET < -\frac{\gamma_{20}}{\gamma_{21}}$;
(M_4^b) $\gamma_{21} < 0, \gamma_{20} < 0$, for all ET;
(M_4^c) $\gamma_{21} < 0, \gamma_{20} > 0, ET > -\frac{\gamma_{20}}{\gamma_{21}}$.

Similarly, if $\alpha > 1, \beta < 1, \gamma_1 > 0$ and one of (M_4^s), $s \in \{a, b, c\}$ are true, X_1^e is the unique positive root for (22).

Case M_5: $\gamma_2 = 0$. When $ET = -\frac{\gamma_{20}}{\gamma_{21}}$, we have $\gamma_2 = 0$. Thus, there exists one positive root X_1^E if $\gamma_3 \cdot \gamma_1 < 0$ and $ET = -\frac{\gamma_{20}}{\gamma_{21}}$. Direct calculation yields that X_1^E is positive if one of the following conditions holds:

(M_5^1)$\gamma_2 = 0, \gamma_3 < 0, \gamma_2 > 0$;
(M_5^2)$\gamma_2 = 0, \gamma_3 > 0, \gamma_2 < 0$.

The detailed conditions can be obtained similarly to Case M_4.

Case M_6: $\Omega = 0$. In this scenario, there exists one root $X_1^F = -\frac{\gamma_2}{2\gamma_3}$. It is easy to see that X_1^F is positive if $\gamma_2 \cdot \gamma_3 < 0$. We denote the conditions for the existence of positive root X_1^F (i.e., $\gamma_0 = 0, \Omega > 0, \gamma_2 \cdot \gamma_3 < 0$) as Case M_6^1.

References

[1] R.L. Siegel, K.D. Miller, A. Goding Sauer, et al., Colorectal cancer statistics, 2020, CA Cancer J. Clin. 70 (2020) 145–164.
[2] H.E. Taitt, Global trends and prostate cancer: A review of incidence, detection, and mortality as influenced by race, ethnicity, and geographic location, Am. J. Men's Health 12 (2018) 1807-šC1823.
[3] W. Zhou, Y. Jiang, L. Ji, et al., Expression profiling of genes in androgen metabolism in androgen-independent prostate cancer cells under an androgen-deprived environment: mechanisms of castration resistance, Int. J. Clin. Exp. Pathol. 9 (2016) 8424–8431.
[4] C. Huggins, C.V. Hodges, Studies on prostatic cancer. I. The effect of castration, of estrogen and of androgen injection on serum phosphatases in metastatic carcinoma of the prostate, Cancer Res. 1 (4) (1941) 293–297.
[5] M.K. Brawer, Hormonal therapy for prostate cancer, Rev. Urol. 8 (2006) S35–47.
[6] N. Spry, L. Kristjanson, B. Hooton, et al., Adverse effects to quality of life arising from treatment can recover with intermittent androgen suppression in men with prostate cancer, Eur. J. Cancer 42 (2006) 1083–1092.
[7] N.D. Shore, E.D. Crawford, Intermittent androgen-deprivation therapy: Redefining the standard of care? Rev. Urol. 12 (2010) 1.
[8] S. Karkampouna, F. La Manna, A. Benjak, et al., Patient-derived xenografts and organoids model therapy response in prostate cancer, Nature Commun. 12 (1) (2021) 1117.
[9] S. Dason, C.B. Allard, J.G. Wang, et al., Intermittent androgen-deprivation therapy for prostate cancer: translating randomized controlled trials into clinical practice, Can. J. Urol. 21 (2014) 28–36.
[10] R. Brady-Nicholls, J.D. Nagy, T.A. Gerke, et al., Prostate-specific antigen dynamics predict individual responses to intermittent androgen deprivation, Nature Commun. 11 (1) (2020) 1–13.
[11] Y. Hirata, K. Morino, K. Akakura, et al., Personalizing androgen suppression for prostate cancer using mathematical modeling, Sci. Rep. UK 8 (1) (2018) 1–8.
[12] S. Pasetto, H. Enderling, R.A. Gatenby, et al., Intermittent hormone therapy models analysis and Bayesian model comparison for prostate cancer, Bull. Math. Biol. 84 (1) (2022) 1–36.
[13] E.M. Rutter, Y. Kuang, Global dynamics of a model of joint hormone treatment with dendritic cell vaccine for prostate cancer, Discrete Contin. Dyn. B 22 (3) (2017) 1001.
[14] T. Phan, K. Nguyen, P. Sharma, et al., The impact of intermittent androgen suppression therapy in prostate cancer modeling, Appl. Sci. 9 (1) (2018) 36.
[15] Z. Wu, T. Phan, J. Baez, et al., Predictability and identifiability assessment of models for prostate cancer under androgen suppression therapy, Math. Biosci. Eng. 16 (5) (2019) 3512–3536.
[16] G. Tanaka, Y. Hirata, S.L. Goldenberg, et al., Mathematical modelling of prostate cancer growth and its application to hormone therapy, Phil. Trans. R. Soc. A 368 (1930) (2010) 5029–5044.
[17] A. Zazoua, W. Wang, Analysis of mathematical model of prostate cancer with androgen-deprivation therapy, Commun. Nonlinear Sci. Numer. Simul. 66 (2019) 41–60.
[18] A. Zazoua, Y. Zhang, W. Wang, Bifurcation analysis of mathematical model of prostate cancer with immunotherapy, Int. J. Bifurcation Chaos 30 (07) (2020) 2030018.
[19] A.M. Ideta, G. Tanaka, T. Takeuchi, et al., A mathematical model of intermittent androgen suppression for prostate cancer, J. Nonlinear Sci. 18 (6) (2008) 593–614.
[20] Y. Pei, Y. Lv, C. Li, et al., Optimization therapy by coupling intermittent androgen suppression with impulsive chemotherapy for a prostate cancer model, Bull. Math. Biol. 85 (12) (2023) 123.
[21] L. Chen, J. Yang, Y. Tan, et al., Threshold dynamics of a stochastic model of intermittent androgen-deprivation therapy for prostate cancer, Commun. Nonlinear Sci. Numer. Simul. 100 (2021) 105856.

[22] J.J. Cunningham, J.S. Brown, R.A. Gatenby, et al., Optimal control to develop therapeutic strategies for metastatic castrate resistant prostate cancer, J. Theoret. Biol. 459 (2018) 67–78.
[23] H. Yoshito, K. Aihara, Ability of intermittent androgen suppression to selectively create a non-trivial periodic orbit for a type of prostate cancer patients, J. Theoret. Biol. 384 (2015) 147–152.
[24] R. Adamiecki, A. Hryniewicz-Jankowska, M.A. Ortiz, et al., In vivo models for prostate cancer research, Cancers 14 (21) (2022) 5321.
[25] V. Sailer, G.von. Amsberg, S. Duensing, et al., Experimental in vitro, ex vivo and in vivo models in prostate cancer research, Nat. Rev. Urol. 20 (3) (2023) 158–178.
[26] A. Filippov, Differential Equations with Discontinuous Righthand Sides, Kluwer Academic, Dordrecht, 1988.
[27] A.F. Filippov, Differential Equations with Discontinuous Righthand Sides: Control Systems, Springer Science Business Media, 2013.
[28] V.I. Utkin, Sliding Modes in Control and Optimization, Springer Science Business Media, 2013.
[29] R. Yan, A. Wang, X. Zhang, et al., Dynamics of a non-smooth model of prostate cancer with intermittent androgen-deprivation therapy, Phys. D 442 (2022) 133522.
[30] T. Zhao, Y. Xiao, R. Smith?, Non-smooth plant disease models with economic thresholds, Math. Biosci. 241 (2013) 34–48.
[31] S. Tang, J. Liang, Y. Xiao, et al., Sliding bifurcations of filippov two stage pest control models with economic thresholds, SIAM J. Appl. Math. 72 (4) (2012) 1061–1080.
[32] A. Wang, Y. Xiao, R. Smith?, Using non-smooth models to determine thresholds for microbial pest management, J. Math. Biol. 78 (2019) 1389–1424.
[33] H. Zhou, S. Tang, Bifurcation dynamics on the sliding vector field of a Filippov ecological system, Appl. Math. Comput. 424 (2022) 127052.
[34] Y. Xiao, X. Xu, S. Tang, Sliding mode control of outbreaks of emerging infectious diseases, Bull. Math. Biol. 74 (10) (2012) 2403–2422.
[35] N.S. Chong, R. Smith?, Modelling avian influenza using Filippov systems to determine culling of infected birds and quarantine, Nonlinear Anal. Real World Appl. 24 (2015) 196–218.
[36] N.S. Chong, B. Dionne, R. Smith?, An avian-only Filippov model incorporating culling of both susceptible and infected birds in combating avian influenza, J. Math. Biol. 73 (3) (2016) 751–784.
[37] C. Chen, N.S. Chong, R. Smith?, A Filippov model describing the effects of media coverage and quarantine on the spread of human influenza, Math. Biosci. 296 (2018) 98–112.
[38] A. Wang, Y. Xiao, R. Smith?, Multiple equilibria in a non-smooth epidemic model with medical-resource constraints, Bull. Math. Biol. 81 (4) (2019) 963–994.
[39] D.C. Vicentin, P.F.A. Mancera, T. Carvalho, et al., Mathematical model of an antiretroviral therapy to HIV via Filippov theory, Appl. Math. Comput. 387 (2020) 125179.
[40] J. Deng, S. Tang, H. Shu, Joint impacts of media, vaccination and treatment on an epidemic Filippov model with application to COVID-19, J. Theoret. Biol. 523 (2021) 110698.
[41] M. Antali, G. Stepan, Sliding and crossing dynamics in extended Filippov systems, SIAM J. Dyn. Syst. 17 (1) (2018) 823–858.
[42] A. Wang, Y. Xiao, R. Smith?, Dynamics of a non-smooth epidemic model with three thresholds, Theory Biosci. 139 (2020) 47–65.
[43] B. Tang, W. Zhao, Sliding dynamics and bifurcations of a Filippov system with nonlinear threshold control, Int. J. Bifurcation Chaos 31 (14) (2021) 2150214.